

Spatial-temporal analysis of blowout dunes in Cape Cod National Seashore using
sequential air photos and LiDAR

by

Kimia Abhar
B.Sc, University of Victoria, 2010

A Thesis Submitted in Partial Fulfillment
of the Requirements for the Degree of

MASTER OF SCIENCE

in the Department of Geography

© Kimia Abhar, 2014
University of Victoria

All rights reserved. This thesis may not be reproduced in whole or in part, by photocopy
or other means, without the permission of the author.

Supervisory Committee

Spatial-temporal analysis of blowout dunes in Cape Cod National Seashore using
sequential air photos and LiDAR

by

Kimia Abhar
B.Sc, University of Victoria, 2010

Supervisory Committee

Dr. Ian J. Walker, University of Victoria, Department of Geography
Supervisor

Dr. Patrick Hesp, University of Victoria, Department of Geography
Supervisory Committee

Abstract

Supervisory Committee

Supervisor

Dr. Ian J. Walker, University of Victoria, Department of Geography

Supervisory Committee

Dr. Patrick Hesp, University of Victoria, Department of Geography

This thesis presents results from spatial-temporal and volumetric change analysis of blowouts on the Cape Cod National Seashore (CCNS) landscape in Massachusetts, USA. The purpose of this study is to use methods of analysing areal and volumetric changes in coastal dunes, specifically blowouts, and to detect patterns of change in order to contribute to the knowledge and literature on blowout evolution.

In Chapter 2.0, the quantitative analysis of blowout change patterns in CCNS was examined at a landscape scale using Spatial-Temporal Analysis of Moving Polygons (STAMP). STAMP runs as an ArcGIS plugin and uses neighbouring year polygon layers of our digitized blowouts from sequential air photo and LiDAR data (1985, 1994, 2000, 2005, 2009, 2011, and 2012 for 30 erosional features, and 1998, 2000, 2007, and 2010 for 10 depositional features).

The results from STAMP and the additional computations provided the following information on the evolution of blowouts: (1) both geometric and movement events occur on CCNS; (2) generation of blowouts in CCNS is greatest in 1985 and is potentially related to vegetation planting campaigns by the Park; (3) features are expanding towards dominant winds from the North West and the South West; (5) the erosional and depositional features are becoming more circular as they develop, (6) the evolution of

CCNS blowouts follows a similar pattern to Gares and Nordstrom's (1995) model with two additional stages: merging or dividing, and re-activation.

In Chapter 3.0, the quantitative analysis of volumetric and areal change of 10 blowouts in CCNS at a landscape scale is examined using airborne LiDAR and air photos. The DEMs of neighbouring years (1998, 2000, 2007, and 2010) were differenced using Geomorphic Change Detection (GCD) software. Areal change was detected by differencing the area of polygons that were manually digitized in ArcGIS. The changes in wind data and vegetation cover were also examined. The results from the GCD and areal change analysis provide the following information on blowout evolution: (1) blowouts generate/initiate; (2) multiple blowouts can merge into an often larger blowout; (3) and blowouts can experience volumetric change with minimal aerial change and vice versa. From the analyzes of hourly Provincetown wind data (1998-2010), it was evident that blowouts developed within all three time intervals. The percentages of comparable winds (above 9.6 m s^{-1}) were highest in 1998, 1999, 2007 and 2010. It is speculated that tropical storms and nor'easters are important drivers in the development of CCNS blowouts. In addition, supervised classifications were run on sequential air photos (1985 to 2009) to analyze vegetation cover. The results indicated an increase in vegetation cover and decrease of active sands over time. Two potential explanations that link increased vegetation to blowout development are: (1) sparse vegetation creates a more conducive environment for the initiation of blowouts by providing stability for the lateral walls, and (2) high wind events (e.g. hurricanes and nor'easters) could cause vegetation removal, allowing for areas of exposed sand for blowout initiation and development.

Table of Contents

Supervisory Committee	ii
Abstract	iii
Table of Contents	v
List of Tables	vii
List of Figures	ix
Acknowledgments	xiii
1.0 Introduction	1
1.1 Research Context	1
1.1.2 Blowout Morphology	1
1.1.3 Remote Sensing and Dune Studies	8
1.1.4 Research Gap	9
1.2 Research Purpose, Objectives, and Thesis Structure	10
2.0 Analyzing the Historical Spatial-Temporal Evolution of Blowouts in Cape Cod National Seashore, Massachusetts, USA	12
2.1 Introduction	12
2.2 Study Area	15
2.3 Data and Methods	17
2.3.1 Data sources	17
2.3.2 Data Accuracy	19
2.3.3 Spatial-Temporal Analysis of Moving Polygons (STAMP) model	20
2.4 Results	29
2.4.1 Erosional Features	29
2.4.2 Depositional features	34
2.4.3 Directional expansion	38
2.4.4 Resultant sand drift potential (RDP) vectors	40
2.5 Discussion	41
2.5.1 Directional Expansion of Blowouts in CCNS	41
2.5.2 Observed Morphological Stages for Blowouts in CCNS	42
2.5.3 Blowout Evolutionary Model	47
2.5.4 Utility of the STAMP method	48
2.5.5 Future Work	49
2.6 Conclusion	50
3.0 Spatial temporal and Volumetric Analysis of Blowouts in Cape Cod National Seashore, Massachusetts, USA	52
3.1 Introduction	52
3.2 Study Area	54
3.3 Data and Methods	56
3.3.1 Data Sources and Pre-processing	56
3.3.2 Volumetric Change Estimates	58
3.3.3 Area Change Calculations	59
3.3.4 Supervised Classification	60
3.3.4 Velocity Threshold	61

3.4 Results	62
3.4.1 Volumetric Change.....	62
3.4.2 Vegetation Change	67
3.4.3 Wind Patterns	68
3.5 Discussion.....	69
3.5.1 Observed morphological and volumetric changes in blowouts of CCNS	69
3.5.2 Drivers of Blowout Development in CCNS	71
3.5.3 Benefits of combining areal and volumetric estimates of geomorphic change	76
3.6 Conclusions	77
4.0 Conclusion.....	80
4.1 Summary and Conclusion.....	80
4.2 Research contributions and future work.....	82
Bibliography	85

List of Tables

Table 1. A list of the source, accuracy, scale, resolution and extent of the orthorectified air photos used in this study to digitize the blowout erosional features.	18
Table 2. A list of the source, accuracy, scale, resolution and extent of the LiDAR used in this study to digitize the blowout erosional and depositional features.	18
Table 3. A breakdown of the total uncertainty calculation of the air photos and digitization that was modified from Mathew <i>et al.</i> (2010). The total uncertainty for airphotos is based on the positional accuracy of the air photos and the onscreen delineation (calculated by repeat trials of outlining polygons).	20
Table 4. A breakdown of the total uncertainty calculation of the LiDAR and digitization that was modified from Mathew <i>et al.</i> , (2010). The total uncertainty for LiDAR is based on the positional accuracy of the air photos and the onscreen delineation of both depositional and erosional features (calculated by repeat trials of outlining polygons). ..	20
Table 5. STAMP typology of events to describe geometric changes in polygons based on overlap relations. The unshaded polygons are from T ₁ and shaded polygons are from T ₂ . The second column shows the modified terms that will be used for the purposes of blowout pattern classification. Same classification scheme and method was used for erosional and depositional lobes.	22
Table 6. STAMP typology of events to describe movement changes in polygons based on proximity relations (a distance threshold set by the user). The unshaded polygons are from T ₁ and shaded polygons are from T ₂ . The second column shows the modified terms that will be used for the purposes of blowout pattern classification. Same classification scheme and method was used for erosional and depositional lobes.	23
Table 7. A table that lists the number of blowout erosional features that experienced spatial-temporal (both geometric and movement) events in the neighbouring T1 and T2 year pairings. These values are results from both STAMP and additional manual computation.	30
Table 8. A table that lists the blowout depositional features that experienced spatial-temporal (both geometric and movement) events in the corresponding T1 and T2 year pairing. These values are results from both STAMP and additional manual computations.	35
Table 9. A list of the source, accuracy, scale, resolution and extent of the orthorectified air photos used in this study to digitize the blowout erosional features.	57

Table 10. A list of the source, horizontal and vertical accuracy, resolution and extent of the LiDAR (obtained from NOAA Coastal Services Center)used in this study to calculate volumetric change of the selected ten blowout erosional and depositional features in CCNS.	57
Table 11. A summary of the change in volume (m^3) as erosion (Eros, -ve values) or deposition (Depo, +ve values) and rate of volumetric change ($m^3 yr^{-1}$) for the subpopulation of 10 blowouts. The greatest rate of net change in volume for all blowouts combined occurred during the 1998-2000 interval, closely followed by the 2000-2007 interval.	63
Table 12. A summary of the V:A ratio for each year and each blowout in the selected sub-population. The volume change was calculated using GCD and the area of expansion was calculated by a differencing of digitized polygons in ArcGIS. These values show that there are instances where blowouts can deepen with minimal change to the lateral walls (e.g. #10 in 2007-2010), expand in area without deepening (e.g. #4 in 1998-2000), as well as both deepen and expand simultaneously (e.g. #10 in 1998-2000).	64

List of Figures

- Figure 1. Wind roses for each season in Cape Cod, Massachusetts are presented. The Winter (December, January and February), Autumn (September, October and November), Spring (March, April and May) and Summer (June, July and August) wind roses (2004–2005) are displayed and the vector sum (black arrow) shows the resultant prevailing winds. The dominant winds, as shown in these roses, are from the North West and South West. 16
- Figure 2. An aerial image from 2009 with a view of the purposed area of study of blowouts in Cape Cod National Seashore, Massachusetts measuring approximately 35 km². There are 30 blowout erosional features and 10 depositional features that have been selected and digitized to view initiation or changes in morphology by disturbance. 17
- Figure 3. The rate of expansion and contraction (m²/yr), as well as the unchanged area (m²) of blowout erosional features. All contraction rate values were given a negative value, as this represents the loss of area in an erosional features. The unchanged area continues to increase over time, showing these features are increasing in size. Expansion rate increases until 2000, quickly decreases from 2000-2009 (with the lowest rate between 2005-2009), and then increases again in the following years. Contraction rate values mirror the expansion rate pattern. These fluctuations in blowout development can be linked to various factors at a landscape scale including increase or decreases in wind speed, precipitation, anthropogenic disturbances, and presence of vegetation. 31
- Figure 4. The rate of area change (m²/yr) within the selected 30 blowout erosional feature subset ($[T2 \text{ area} - T1 \text{ area}] / \text{number of years between T1 and T2}$). The rate of area change follows the same pattern as the expansion rate. Variations of these values over time can be linked to various factors at a landscape scale including increases or decreases in wind speed, precipitation, anthropogenic disturbances, and presence of vegetation. 31
- Figure 5. The shape metric values for each erosional blowout feature in a particular year with a line (black) that represents the mean value for each year. The average of the shape metric shows a steady increase in value, which indicates the blowouts are getting larger and more circular/less complex in shape. It is important, however, to examine the shape metric of individual blowouts (see figure 6). 32

Figure 6. The shape metric values over time for a selected subset of 15 blowouts from the original 30 dataset to discern shape patterns in individual erosional features of the sub-population. The shape metrics of individual features show that erosional hollows are either: (1) steadily increasing, (2) following the same pattern of the rate of area change (increase, decrease and increase), or (3) have an overall decrease in shape metric (i.e. more complex and less circular).....32

Figure 7. Examples of blowout erosional feature shapes over time as observed by shape metric values and observations during digitization. (a) The erosional feature shape becomes less complicated over time (an increase in area and decrease in perimeter value, which indicates an increase in shape metric over time), which represents an active blowout; (b) The erosional feature shape becomes less complicated and more circular from 1994-2005 (active blowout), then becomes less circular from 2005-2009 (vegetation encroachment), and in 2011 there is an increase in area (removal of vegetation and erosion).33

Figure 8. A list of union (blowouts merging) and division (blowouts break into double or multiples) events that occurred in the sequence of airphotos and LiDAR, as well as examples of these events over time. (A) The table on the left is a list of all the union events that occurred in the sequence, and to the right is an example of a union event that occurred as a result of a clustering and expansion events. (B) The table on the left lists the single division event that occurred in the sequence, and to the right is an example of a division event that is followed by contraction events.34

Figure 9. The rate of expansion and contraction (m^2/yr), as well as the unchanged area (m^2) of blowout depositional features. All contraction rate values were given a negative value, as this represents the loss of area in erosional features. The unchanged area experiences a decrease in 2000-2007 followed by an increase in 2007-2010, which shows that these features experience variability in their shape over time. The expansion rate and contraction rate are again mirrored and show that the rate of development of these features decreased in 2000-2007, but drastically increased from 2007-2010.35

Figure 10. The rate of area change within the selected 10 blowout depositional feature subset ($[T2 \text{ area} - T1 \text{ area}]/\text{number of years between T1 and T2}$). The negative values reveal that the total area of T1 blowouts is greater than the total area of T2 blowouts. These values show that although change in shape may have been occurring, the area of these features did not increase 1998-2007, but from 2007-2010 there was a drastic increase in area change.36

Figure 11. The shape metric values for each blowout depositional feature in a particular year with a line (black) that represents the mean value for each year. The average value indicates that these features become more complex in shape before they expand radially and become more circular.37

- Figure 12. The shape metric values over time for a selected subset of 5 blowout depositional features to discern shape patterns in individual features of the population. These value indicates that these features become more complex in shape before they expand radially and become more circular.....37
- Figure 13. Example of depositional feature shape over time in CCNS. Although the depositional lobes display variety in their morphology over time, the majority of depositional lobes have a similar pattern of evolution; an initial decrease in shape metric followed by an increase in shape metric, which indicates an increase in area and a decrease in perimeter (indicative of a less complicated shape). T1 is outlined and T2 is solid, as well each year has a corresponding colour (1998=red, 2000=blue, 2005=green, and 2010=orange). The black lines represent the area of the blowout hollow.....38
- Figure 14. Distribution of the direction of expansion of erosional features from 1985-2012. The length of the black bar corresponds to the sum of the area of expansion in each direction. The red arrow is the resultant direction of expansion. (A) The display of expansion divided into four cardinal directions output by STAMP. (B) The display of expansion divided into eight cardinal directions output manually by computations in ArcGIS. Both roses show that erosional features in CCNS are expanding in the direction of the dominant winds towards ENE, ESE and SSE.39
- Figure 15. Distribution of the direction of expansion of depositional features from 1998-2010. The length of the black bar corresponds to the sum of the area of expansion in each direction. The red arrow is the resultant direction of expansion. (A) The display of expansion divided into four cardinal directions output by STAMP. (B) The display of expansion divided into eight cardinal directions output manually by computations in ArcGIS. Both roses show that the depositional feaures in CCNS are expanding in the direction of the dominant winds towards the ENE and SSE.39
- Figure 16. Sediment drift roses created using the Fryberger and Dean (1979) method. (A) An annual sediment drift rose with the resultant indicating sand being dominantly transported towards the SSE (155°) (B) Seasonal sediment drift roses indicating that in Fall, Winter and Spring the dominant direction of sediment transport is towards the SSE and in Summer is towards the SSW.40
- Figure 17. An aerial image from 2009 with a view of the proposed area of study of blowouts in Cape Cod National Seashore, Massachusetts measuring approximately 35 km². Ten blowouts were selected and digitized to analyze volumetric and aerial changes.55
- Figure 18. An example of a blowout (not included in sub-population) generation between 2000-2007 (bottom right corner of air photo), and development of a pre-existing blowout (#1). The V:A ratio shows that the greatest erosion occurred between 1998-200065

- Figure 19. An example of a union event where multiple blowouts (#6) expand into one larger feature (examples seen in STAMP 2D analysis of CCNS blowouts (Abhar *et al.*, 2014). The union event occurs sometime between 2000-2007, which again shows the greatest degree of total change (erosion plus deposition rates) potentially due to Hurricane Noel. (Red = Erosion and Blue = Deposition). 66
- Figure 20. An example of a blowout (#8) increasing in depth, but not in area in 2000-2007. In 2007-2010, however, the feature experiences an increase in area. (Red = Erosion and Blue = Deposition). 67
- Figure 21. Percentage of surface classified as active sand, sparse vegetation (grassy/ammophila), and dense vegetation (shrubs and trees) as calculated by a supervised classification in ENVI. Over time there is a decrease in active sand surfaces, where the dense and sparse vegetation increase. 68
- Figure 22. The percentage of wind data above the Bagnold derived threshold of 9.6 m s^{-1} graphed for each year. Hurricane years of 1998 and 1999 had the greatest percentage of competent winds, followed closely by 2007 and 2010. These periods correspond with the greatest rates of erosion of blowouts in the 10 blowouts measured in the Cape Cod region. 69
- Figure 23. An example of patches of bare sand in CCNS that have formed by vegetation die-back, failure to thrive, or some other currently unknown mechanism. Although there are many factors that could have contributed to the removal of vegetation, or lack of it within a certain patch, high wind events are drivers of vegetation burial and removal. These sparsely vegetated patches, which are widely present on the CCNS landscape, are conducive to blowout initiation. (Image source: Patrick Hesp, October 2012). 76

Acknowledgments

I would like to thank my supervisors Dr. Ian J. Walker and Dr. Patrick Hesp for all of their support and guidance during these years.

Thank you to my CEDD lab mates for their help and laughs.

Thank you to my parents, brother and friends for their constant love and support.

Thank you to my partner, Dylan, for always staying up too.

1.0 Introduction

1.1 Research Context

This research explores the spatial-temporal evolution of aeolian blowout dunes by tracking decadal scale changes in their areal and volumetric changes as a means to improve our understanding of blowout initiation, evolution, and morphodynamics at Cape Cod National Seashore (CCNS), Massachusetts, USA; which hosts one of the highest densities of blowouts, of varying morphology, in the world. Although these features are the most common aeolian land features in desert and coastal dune landscapes, there are few studies that have explored the morphodynamics of blowout dunes (Hesp, 2002). The proposed research, therefore, will significantly increase and contribute to our understanding of blowout initiative, evolution and morphodynamics.

1.1.2 Blowout Morphology

I. Blowout definition and type

The blowout landform was first mentioned in the literature by Cowles (1898) who described them as ‘trough shaped wind sweeps’. However, the actual term ‘blowout’ gained scientific acceptance when Melton (1940) used them to describe parabolic dunes that were arising from the deflation of sand surfaces on the semi-arid dunelands of the southern High Plains. Bagnold (1941) defined the term further as wind-scoured gaps in an otherwise continuous transverse dune, and his definition has now been accepted as the common used term through concurrent works. Blowouts are saucer, cup or trough-shaped depressions or hollows that evolve by aeolian erosional forces on partially vegetated pre-

existing sand deposit or dune complex in semiarid to hyper-arid environments (Carter *et al.*, 1990; Byrne 1997; Hesp and Hyde, 1996; Hesp, 2002; Hugenholtz and Wolfe, 2006; Smyth *et al.*, 2012).

Various types of blowouts have been identified in the literature and their classification is based on their variable morphology. Examples include those of Ritchie (1972), who defined four types/shapes of blowouts: cigar-shaped; v-shaped; scooped hollow; and cauldron/corridor, as well as Smith (1960) who suggested that blowouts ranged from pits to elongated notched, troughs or broad basins. Two primary types of blowouts defined by Cooper (1958, 1967), trough and saucer blowouts, are used commonly to classify a large variety of blowouts (Hesp, 2002). The trough blowout is characterized as being generally more elongated, having steeper and longer erosional walls, and having deeper deflation floors and basins. The saucer blowout, on the other hand, is characterized as being semicircular or saucer-shaped and described as shallow dishes. The varied morphologies of blowouts also reflect the spatial and temporal variability of these erosional features. Smith (1960) observed that shallow saucer blowouts were initiated on the broad crests of foredunes and elongated trough blowouts were initiated on steep stoss faces of dunes. This observation was also noted in the dunefields of Australia and New Zealand by Carter *et al.* (1990). However, there are several factors that control the initial shape, size, location, and evolution of blowouts. There are still many environments where it is not yet understood why one blowout type is present over the other (Hesp, 2002).

II. Blowout Initiation

Blowouts form readily in dune terrain and are common in coastal environments where either stable or unstable morphologies exist (Nordstrom *et al.*, 1990). They occur where vegetated dunes (particularly foredunes) are eroding, but also in stable and accretionary environments with high wind and wave energy (Hesp, 2002).

There are various factors that can potentially initiate the development of a blowout, including: (1) acceleration of wind where scarping of the seaward face of the foredune has occurred due to wave erosion, (2) climatic variability and drought, (3) topography and resulting secondary airflow accelerations, (4) vegetation die-back and encroachment over space and time, (5) high velocity wind erosion, sand inundation and burial, (6) diverse intrusive human activities, (7) and natural nutrient depletion and soil surface disintegration (Hesp, 2002).

Wave erosion that occurs continuously along the shore causes scarp slumping of foredunes. This erosional process couples with airflow acceleration on potentially semi-vegetated slumped surface and can result in the development of a blowout (Hesp, 1982). Wave scarping may also cause complete removal of vegetation, which then exposes the bare surface sediment to potential aeolian erosion and blowout development (Hesp and Hyde, 1996). As well, if vegetation cover does not begin to encroach in a sufficient time period, the hollows and fans that are created due to overwash may develop into blowouts (Hesp, 2002).

Climate variability is a strong factor in initiating blowouts, both in the past and is expected to continue to do so in the future (Hesp, 2002). In periods of prolonged aridity, for example, vegetation cover on the surface is reduced or completely removed due to the

lack of moisture, which leaves the sand surface exposed to potential aeolian erosion and blowouts may be initiated (Thom *et al.*, 1994). Furthermore, climatic phases, such as the El Niño – Southern Oscillation (ENSO), can play a role in wind erosion potential. For example, in 1991 in New Zealand, the westerly winds were much stronger than average during the El Niño, and it was observed that the evolution of blowouts was greater compared to subsequent years (Hesp, 2002). Similarly, very high velocity winds and hurricanes can manipulate the vegetation cover of a surface by removing, undermining, eroding, and burying it. This will initiate blowouts as the bare surface is once again exposed to erosional processes (Hesp, 2002).

Topographic acceleration of wind flow over scarps, cliffs, and bowl-shaped topography is an essential process in the development of blowouts. However, topography can also be a factor that initiates blowouts as well (Hesp, 2002). For example, blowouts are systematically formed on the downwind edge of cliffs in the Head of Bright region in southern Australia where the cliffs were high, curved, and embayed (Hesp and Hyde, 1996).

Vegetation encroachment and die-back can occur on sandy surfaces over time and space, which can also contribute to blowout initiation (e.g., Nordstrom and Gares, 1995). The loss of vegetation on a surface can result from soil nutrient depletion, localized aridity, animals burying or removing vegetation, and high wind events also burying and removing vegetation. Without vegetation to trap sediment supply and to reduce wind acceleration, sandy surfaces are exposed to aeolian erosion and blowouts may initiate (Hesp, 2002).

Human activities, are also considered an important factor in blowout initiation, as they result in the removal of vegetation and/or sediment supply from the surface. These include activities such as pedestrian trampling, creating walking trails, offroad vehicle activity and roads, fencing and building development, military training, and fires (Nordstrom *et al.*, 1990; Hesp, 2002).

III. Blowout flow dynamics/sand transport

Once a blowout has been initiated, it will typically develop and increase in size through erosion of the deflation basin and slumping of the slope or side walls (Nordstrom *et al.*, 1990). Blowouts enlarge laterally by wind scour, which causes the side walls to oversteepen and that causes avalanching. Vertical changes also occur by deflation of the blowout floor and growth and migration of the depositional lobe (Nordstrom *et al.*, 1990).

As indicated by Olson (1958), blowout development involves wind flows that are topographically accelerated and steered, where flow separation is common over lee slopes and, in some circumstances, where concentrated regions of accelerated flow occur. (Hesp, 2002, Nordstrom *et al.*, 1990, Hugenholtz *et al.*, 2006, Smyth *et al.*, 2013). Hesp and Hyde (1996) examined the flow dynamics and related sand transport patterns in a trough blowout and observed that during oblique approach winds, there was significant topographic steering by the erosional walls, high speed flow along the deflation basin, and lateral erosion toward the wall crests. Flow deceleration occurred rapidly over the depositional lobe in response to lateral expansion and flow separation. These flow patterns occur where the boundary layer separates from the surface due to movement along an adverse pressure gradient, which can also result in flow reversal in the form of eddies and vortices (Nordstrom *et al.*, 1990).

Jugarius et al. (1981) conducted a study on six blowouts (mostly saucers) near Noordwijkerhout in the Netherlands and observed surface changes over a period of two years and at 80 erosion pin sites. The authors concluded that there was great complexity in sand erosion and deposition in blowouts due to varying wind speeds and directions, as well as other climatic factors. They also concluded that the multi-directional characteristics of the winds were driving the circular shape of the saucer blowouts.

Other climatic factors, such as seasonality, also play a role in blowout morphodynamics. While studying relationships between deflation in saucer blowouts and near surface winds at Meijendel in the Netherlands, Pluis (1992) found that less erosion occurred in the winter months when wind was high due to higher surface moisture levels compared to drier summer months. In another study by Byrne (1997), seasonal sand transport patterns in a blowout on Lake Huron in Ontario were found to be greatest in winter and fall due to dormancy and die-back of vegetation; and that spring and summer months were generally more accretionary. Therefore, the change of seasons adds another layer of complexity when determining the impact of wind flow action on blowout dunes.

IV. Evolution/Geomorphology

After initiation, a blowout continues to evolve and enlarge as the side walls recede, the deflation basin deepens, and the depositional lobe grows and extends. Blowouts can evolve in numerous ways and the pattern of development depends on the following factors: wind speeds; dominant wind direction(s); vegetation type, density, and the potential for revegetation; beach processes and current state (receding, stable or prograding); and the magnitude and frequency of storm and erosion events (Hesp, 2002). Sand supply and the depth to which a blowout can develop are also controlled by factors

including fluctuating water table levels, depth to erosion-resistant surfaces (e.g., calcrete layers) or developed lag surfaces (e.g., pebble, shell, pumice, or artifact residuals, e.g., Ritchie 1972, Hesp 2002, Nordstrom *et al.*, 1990). Blowouts can also become too wide and impede the creation of accelerated flows that transport sand. In shallow saucer blowouts, however, the flow decelerates in the deflation base (Hesp, 2002).

The lateral evolution of a blowout follows a general pattern. When the upper slopes of a blowout are partially or fully vegetated, the process of blowout evolution follows the pattern of unvegetated slope sediment removal, oversteepening of the erosional wall, then slumping (a form of mass wasting), and the walls then retreat (Gares, 1992). As a result of flow within the deflation basin, the slumped sediment is then removed downwind. Saucer blowouts, compared to trough blowouts, are more likely to expand upwind by reversing flows over the surrounding erosional walls, which lead to undermining, wall collapse and retreat (Hesp, 2002). There is increased complexity in blowout formation and wind flow with slumping blocks, debris slopes, vegetation stumps, and fallen logs.

The orientation at which blowouts evolve can be influenced by the variability of the strength and direction of regional approach winds. Trough blowouts often have a skewed orientation due to erosion occurring on one erosional wall. This is a result of oblique approach wind (Byrne, 1997). In saucer blowouts, flow separation occurs on walls and erosion occurs around the crests of the walls. The expansion of blowouts can potentially occur in various locations as a result of regional wind conditions, which flow in various directions (Hesp, 2002). Although some blowout evolutionary trends have been identified in the literature, there is still a great need for further understanding, which can be investigated using sequential air photos and LiDAR data.

1.1.3 Remote Sensing and Dune Studies

The use of remotely sensed data to investigate the spatial and temporal patterns of change in dune landscapes is increasing (e.g., Woolard and Colby, 2002; Mitasova *et al.*, 2005; Dech *et al.*, 2005; Hugenholtz and Wolfe, 2005; Hugenholtz *et al.*, 2009; Hugenholtz and Barchyn, 2010; Mathew *et al.*, 2010; Eamer and Walker, 2010; Hamilton *et al.*, 2001; Smyth 2012 and 201; Darke *et al.* 2013). As noted by Hugenholtz *et al.* (2012), there has been an evolution of the use of remotely sensed data and dune studies. Earlier studies involving remotely sensed imagery were aiming to map and classify locations, vegetation species, and wind directional variability (Fryberger, 1979; Mackee, 1979; Wasson and Hyde, 1983). As technology progressed there was a shift to using these data types for studying characteristics of dune surfaces (Jungerius and van der Meulen, 1989; Paisley *et al.*, 1991; Lancaster *et al.*, 1992; Walden and White, 1997; Pease *et al.*, 1999). Presently (i.e., over the last decade), there has been the additional use of remotely sensed data to quantitatively analyze areal and volumetric changes to analyze dune morphodynamics and evolution. As well, the larger scale information provided by remotely sensed data has allowed for more dunefield-scale studies that use spatial analysis of dune activity, patterns of change and landscape interactions (Hugenholtz and Wolfe, 2005; Hugenholtz *et al.*, 2009; Hugenholtz and Barchyn, 2010; Eamer and Walker, 2010; Darke *et al.*, 2013; Eamer and Walker, 2013; Abhar *et al.*, 2014, in review).

The use of geographical information systems (GIS) to analyze remotely sensed data, such as aerial photography and LiDAR-derived digital elevation models (DEMs), allows analyzes at larger spatial and temporal scales, which provides great opportunities

to examine blowout morphodynamics (e.g., Dech *et al.*, 2005). Analysis of repeat DEMs (derived from aerial photography or LiDAR) and sequential air photos, for example, allow multi-temporal investigation of spatial patterns in blowout areas and volumes as they evolve. There have been advancements in both the data and software that allowed for the development of methods to detect and quantify spatial-temporal changes in both raster (e.g., Wheaton *et al.* 2010) and polygonal datasets (e.g., Robertson *et al.*, 2007).

1.1.4 Research Gap

As indicated above, our understanding of blowouts as landscape features is still limited. Hesp (2002) stated five areas of research that would contribute to the knowledge base of blowouts: (1) research on the various controlling factors of blowout type and morphological evolutions such as topographic positioning, wind regime, wind directional variability, and vegetation cover and species; 2) the effects of different wind regimes and vegetation communities on the rate of blowout erosion and movement; (3) comparative studies on blowout evolution, dynamics and migration rates in different settings (e.g., windy, low energy, eroding, stable and accreting coasts; and (4) development of comprehensive models of evolution that consider common patterns of change in blowout features.

Jungerius and van der Meulen (1989) suggested that further analysis of blowout evolution through air photo and landscape reconstruction can be done through the use of GIS to allow for investigation of pattern analysis. As stated by Hugenholtz (2013), spatial-temporal analysis of dune features at a landscape scale are becoming more and more prominent in literature, and this approach can assist in developing evolution models of features, such as blowouts. By addressing these knowledge gaps, it is anticipated that

the general change patterns and evolution of blowouts will be identified. This information can be used in parks management practices, as well the features can be used as indicators of landscape change.

1.2 Research Purpose, Objectives, and Thesis Structure

This thesis is structured around two result sections (Chapters 2 and 3) that focus on: i) 2-dimensional pattern analysis of erosional and depositional features of blowouts in CCNS and ii) areal and volumetric change analysis of ten CCNS blowouts. These sections are bookended with an Introduction (Chapter 1) that sets the research context and Conclusions (Chapter 4) that reviews key findings of the research.

The general purpose of this research is to garner a better understanding of blowout evolution by using and applying two existing methodologies, which have not previously been used for measuring geomorphic change, for detecting patterns of two and three-dimensional change. The purpose of section 2 is to identify and analyze spatial-temporal change patterns in two dimensions of blowout features in CCNS using a spatial pattern detection and analysis method known as Spatial-Temporal Analysis of Moving Polygons (STAMP) developed by Robertson *et al.* (2007). The erosional features and depositional lobes of blowouts are digitized in each year of the series and compared against the neighbouring year polygons to extract spatial-temporal patterns and quantifiable metrics that describe movement and change. The specific objectives of this section are: (1) to identify and digitize 30 erosional features from the sequential orthophotography and LiDAR and 10 depositional features from the LiDAR with different stages of evolution and types of morphology to have a representative sub-population, (2) to analyze spatial-temporal patterns within the populations of blowout

features using the STAMP method, (3) to include more geomorphically-relevant categories and measures with the STAMP method to describe changes in blowouts more effectively. This section has been submitted as a manuscript for peer review to the journal *Geomorphology*, and is currently in revision (February, 2014).

The purpose of section 3 is to identify ten representative blowouts in CCNS and calculate the volumetric changes using Wheaton et al. (2010) Geomorphic Change Detection (GCD) software and LiDAR data, as well to calculate the areal expansion over time to allow for both a three and two dimensional analysis of blowout evolution. GCD, which is a DEM differencing software, was primarily developed for the purpose of calculating morphological change detection and sediment budgeting of river systems. The specific objectives of this section are: (1) to calculate the volumetric and areal changes in the selected sub-population of ten blowouts in GCD and GIS using LiDAR (1998, 2000, 2007, and 2010) to further understand the evolution of blowouts in CCNS, (2) to quantify changes in vegetation and active sand cover over time by running supervised classifications of air photos (1985, 1994, 2001, 2005, 2009) to assist in understanding morphological changes of blowouts seen in two and three dimensional analysis, (3) to calculate the percentage of winds in CCNS above the velocity threshold between 1998 and 2010 to understand morphological changes seen in two and three dimensional analysis. This section is a revised draft of a manuscript for submission for peer review to the journal *Geomorphology*.

2.0 Analyzing the Historical Spatial-Temporal Evolution of Blowouts in Cape Cod National Seashore, Massachusetts, USA

2.1 Introduction

This paper explores the spatial-temporal evolution of aeolian blowout dunes by tracking decadal scale changes in their morphology as a means to improve our understanding of blowout initiation, evolution, and morphology. Blowouts occur in coastal and continental environments as well as high to low latitudes, and are commonly described as depressions, hollows, and troughs that form in preexisting sand deposits by aeolian erosion (Carter *et al.*, 1990; Byrne 1997; Hesp and Hyde, 1996; Hesp, 2002; Hugenholtz and Wolfe, 2006). Blowouts are generally categorized by their morphology, which is variable and includes saucer, cup/bowl, or trough shaped forms. Saucer blowouts are described as semi-circular, shallow, dish-shaped depressions. Deeper cup- or bowl-shaped blowouts often evolve from saucer forms. Trough blowouts have steeper, longer erosional lateral walls, generally deeper deflation basins, and commonly more defined depositional lobes (Hesp, 2002). Although formed by erosion, blowouts also have an associated depositional lobe and, thus, they are composed of both erosional and depositional features (Gares and Nordstrom, 1995). The development of blowouts is facilitated and limited by factors such as dominant wind speed and direction, sand inundation and burial, topography, vegetation cover and variation through space and time, climatic variability, water and wave erosion, and land use change by human activities (e.g., Gares and Nordstrom, 1995; Hesp 2002; Smyth et al., 2012, 2013). However, the main driving force controlling blowout size, shape, and direction of

expansion is the wind regime and resulting complex flow dynamics within blowouts that promote and maintain erosion (e.g., Landsberg, 1956; Cooper, 1958; Jungerius *et al.*, 1981; Gares and Nordstrom, 1995; Hesp, 2002; Smyth *et al.*, 2012, 2013; Hesp and Walker, 2013). Jungerius *et al.* (1981) found that although sand erosion and deposition in blowouts in De Blink, Netherlands was complex due to varying wind speeds and directions, blowouts commonly grew in length upwind against the prevailing wind.

Although blowouts are common aeolian features in desert and coastal dune landscapes, there are relatively few studies of their morphodynamics and development (Hesp and Hyde, 1996; Hesp, 2002; Hugenholtz and Wolfe, 2006; Hesp, 2011; Smyth *et al.*, 2013). Blowout development has been linked to changes in climate and human activity. However, without comprehensive knowledge and systematic methods to study their evolution, these features cannot be used as clear indicators of change for purposes of conservation, restoration, and management of parks and protected areas such as the Cape Cod National Seashore.

Increasingly, spatial-temporal patterns of change are being examined in geomorphology to monitor the evolution of features on varying landscapes, including aeolian blowouts and parabolic dunes (e.g., Woolard and Colby, 2002; Mitasova *et al.*, 2005; Dech *et al.*, 2005; Hugenholtz and Wolfe, 2005; Hugenholtz *et al.*, 2009; Hugenholtz and Barchyn, 2010; Mathew *et al.*, 2010). The use of geographical information systems (GIS) to analyze remotely sensed data, such as aerial photography and LiDAR-derived digital elevation models (DEMs), allows analyzes at larger spatial and temporal scales, which provides great opportunities to examine blowout

morphodynamics (Dech *et al.*, 2005). Analysis of repeat DEMs, for example, derived from aerial photography or LiDAR allow multi-temporal investigation of spatial patterns in blowout areas and volumes as they evolve. Until recently, GIS methods were limited in their ability to represent and analyze spatial-temporal patterns and changes, as each data layer was representative of a single temporal series and the links between series were not supported. More recently, however, methods have been developed to specifically detect and quantify spatial-temporal changes in both raster (e.g., Wheaton *et al.* 2010) and polygonal datasets (e.g., Robertson *et al.*, 2007).

The purpose of this study is to identify and analyze spatial-temporal patterns in blowout features in CCNS using a recent spatial pattern detection and analysis method known as Spatial-Temporal Analysis of Moving Polygons (STAMP) developed by Robertson *et al.* (2007). STAMP allows for pattern-based detection, quantification, and representation of changes that occur through time and space using polygons. The STAMP program expands upon Sadahiro and Umemura's (2001) original changing polygon distribution method by including moving and overlapping polygons. In the case of blowouts, erosional features and depositional lobes of blowouts are digitized (identified in earliest year and tracked back through time) in each year of the series and compared against the neighbouring year polygons to extract spatial-temporal patterns and quantifiable metrics that describe movement and change.

Specific objectives of this paper include: (1) to identify 30 erosional features from digital orthophotography and LiDAR between 1985 to 2012 and 10 depositional lobes from more limited LiDAR data between 1998 and 2010 that have experienced notable geomorphic change within the Provincelands region of CCNS, (2) to analyze spatial-

temporal patterns within the populations of blowout features using the STAMP method, (3) to modify and expand the STAMP method to include more geomorphically-relevant categories and measures that describe changes in blowouts more effectively, and (4) to assess if STAMP and the modifications made to the method are appropriate for describing the evolution of blowouts in CCNS. The results of this study will allow for a better understanding of blowout evolution and present a method (STAMP) of exploring these patterns using remotely sensed data and spatial-temporal analytical methods.

2.2 Study Area

Cape Cod National Seashore (CCNS) is a protected area managed by the U.S. National Parks Service (NPS) that encompasses 176 km² of beach and upland landscapes on Cape Cod, Massachusetts, USA (Fig 1). CCNS hosts one of the highest densities of saucer and bowl blowouts in the world. The outer cape region between Provincetown and Orleans was formed over 20,000 years ago by glacial melt-water deposits that drained westward from the South Channel Lobe into Glacial Lake Cape Cod. Following glacier retreat, the Provincelands hook formed approximately 6,000 years ago from eroded glacial drift sediments and sandy marine deposits that travelled northward in littoral drift (Zeigler *et al.*, 1965). Strong regional winds further shaped the Provincelands area by the development of large parabolic dunes, foredunes, and blowouts on top of the former mid-Holocene deposits. These dunes have since been exposed to both anthropogenic disturbance and reclamation (e.g., replanting and stabilization efforts) over the years. Currently, the vegetated areas of the landscape are dominated by American beach grass (*Ammophila breviligulata*), which is an effective agent in controlling the vertical accretion and horizontal movement of coastal dunes and blowouts (e.g., Maun,

1998; Maun and Perumal, 1999). Regional climate and wind patterns are also dominant driving forces in the morphodynamics of dune systems in CCNS. Mean annual precipitation is 106.5 cm (NOAA, 2002) and the wind regime (Figure 1) is seasonally bi-directional with modes from the northwest and southwest.

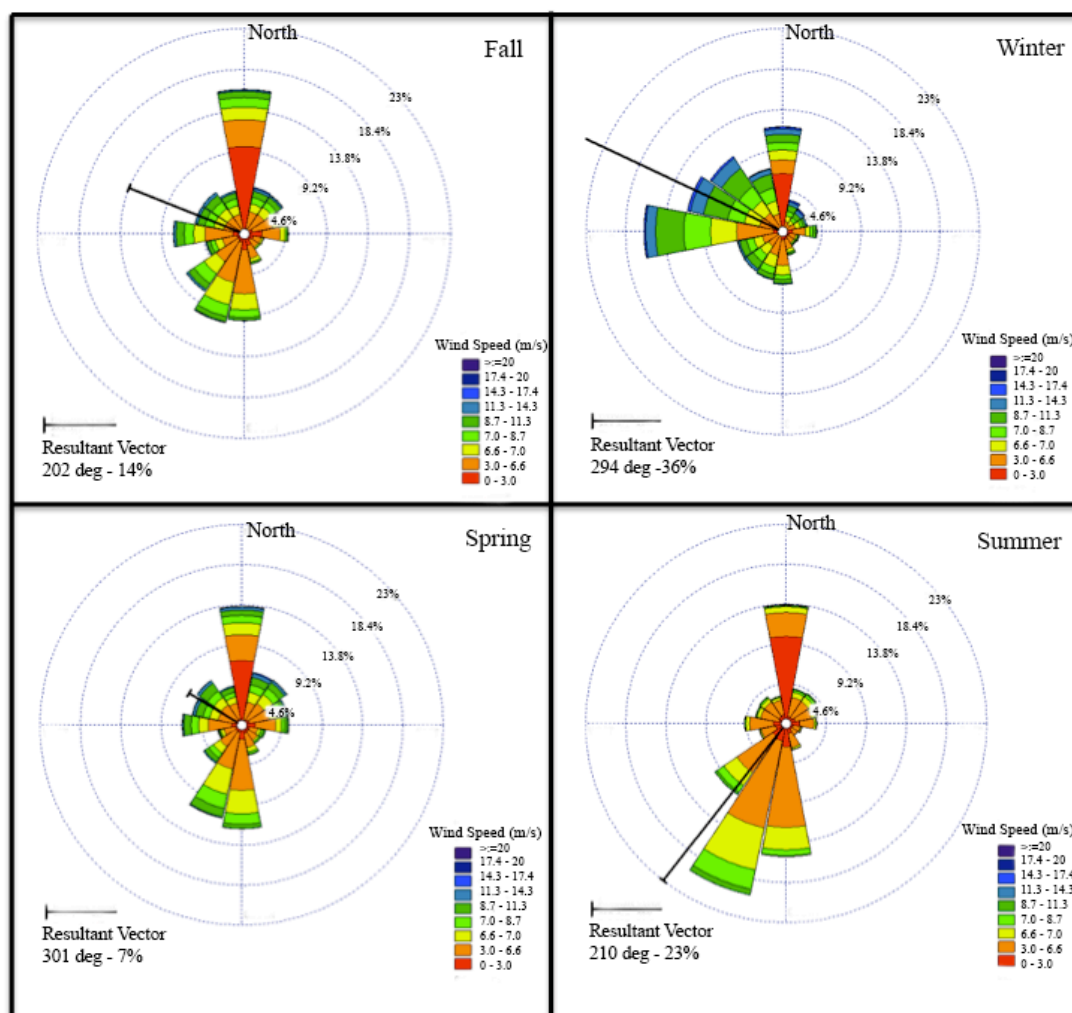


Figure 1. Wind roses for each season in Cape Cod, Massachusetts are presented. The Winter (December, January and February), Autumn (September, October and November), Spring (March, April and May) and Summer (June, July and August) wind roses (2004–2005) are displayed and the vector sum (black arrow) shows the resultant prevailing winds. The dominant winds, as shown in these roses, are from the North West and South West.

The Provincelands dune fields are a prominent and geomorphically distinct region in the landscape of CCNS and cover approximately 35 km² of the park, as seen in Figure

2. As noted by Forman *et al.* (2008), there are at least eleven discrete parabolic dunes with distinct arms and depositional lobes in this landscape and most of these are being reworked to various degrees by contemporary blowout development. This is the location where 30 erosional features and 10 depositional features were found across the CCNS are analyzed for their evolution (see Figure 2). Given the diversity of blowout features with varying shapes, sizes, and stages of development coupled with the broader landscape, wind and land use variability, and plentiful record of aerial photography and LiDAR, the CCNS region presents a prime study area for spatial-temporal analysis of blowouts.

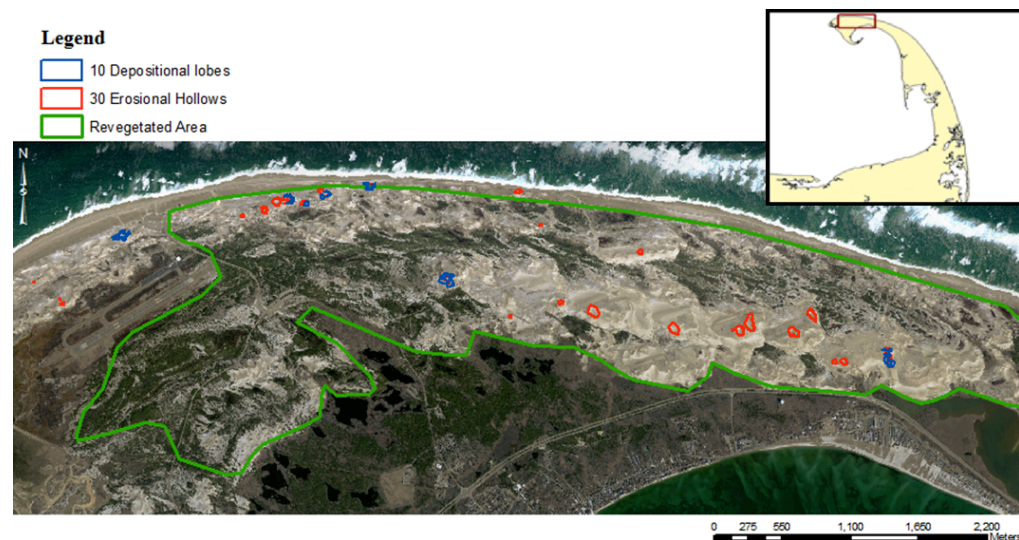


Figure 2. An aerial image from 2009 with a view of the purposed area of study of blowouts in Cape Cod National Seashore, Massachusetts measuring approximately 35 km². There are 30 blowout erosional features and 10 depositional features that have been selected and digitized to view initiation or changes in morphology by disturbance.

2.3 Data and Methods

2.3.1 Data sources

Series of orthorectified air photos and LiDAR data for the CCNS region were obtained from CCNS staff, the State of Massachusetts Office of Geographic Information (MassGIS) (Massachusetts Office of Geographic Information, 2013), and the National Oceanic and Atmospheric Administration online data access viewer (NOAA Coastal

Services Center, 2013). The orthophotography used in analysis was from 1985, 1994, 2007, 2009, 2011, 2012 (Table 1), whereas the LiDAR data was more temporally limited from 1998, 2000, 2007, and 2010 (Table 2). Both datasets were assessed for their post-processed quality for identifying and assessing blowouts in CCNS by reviewing their positional accuracy between years, as well as horizontal accuracy of the LiDAR data.

Year	Source	Horizontal Accuracy (m)	Scale	Pixel Resolution (m)	Extent
1985 (BW)	USDA	> 3	1:60,000	1	Entire Provincelands
1994 (BW)	MassGIS	> 3	1:10,000	0.5	Entire Provincelands
2005 (Coloured)	MassGIS	> 3	1:5,000	0.5	Entire Provincelands
2009 (Coloured)	MassGIS	> 3	1:5,000	0.3	Entire Provincelands
2011 (Coloured)	NOAA (IOCM)	> 1.5	1:2500	0.5	Entire Provincelands
2012 (Coloured)	NAIP	> 1.5	1:20,000	1	Entire Provincelands

Table 1. A list of the source, accuracy, scale, resolution and extent of the orthorectified air photos used in this study to digitize the blowout erosional features.

Year	Division	Horizontal Accuracy (cm)	Vertical Accuracy (cm)	Nominal Ground Spacing (m)	Extent
1998	NOAA Coastal Services Center	> 80	>15	1	Entire Provincelands
2000	NOAA Coastal Services Center	> 80	>15	1	Entire Provincelands
2007	NOAA Coastal Services Center	> 75	>20	1	Entire Provincelands
2010	NOAA Coastal Services Center	> 75	>20	1	Entire Provincelands

Table 2. A list of the source, accuracy, scale, resolution and extent of the LiDAR used in this study to digitize the blowout erosional and depositional features.

Wind data for the Provincetown region was obtained from the National Climate Data Center for years between 1991 and 2012 (National Climatic Data Center, 2013).

Using these data, aeolian sediment drift potential roses were derived using Fryberger and Dean's (1979) method. Regional wind roses and frequency tables for the drift roses were derived using Lakes Environment's WR Plot software.

2.3.2 Data Accuracy

In order to define uncertainty and accuracy issues for analyzing two-dimensional spatial data, a modified error and total uncertainty calculation used by Mathew *et al.* (2010) was implemented for both LiDAR and orthophoto datasets. In this method, two types of uncertainty were accounted for: positional and measurement (Stojic *et al.*, 1998; Moore, 2000; Fletcher *et al.*, 2003; Mathew *et al.*, 2010). The total uncertainty for LiDAR and orthophoto datasets were based on the sum of the horizontal accuracy and the onscreen delineation for each data set in the individual years (Tables 3 and 4). The horizontal accuracy is based on the position of a certain location on the image compared to the same georeferenced location on the Earth's surface. The onscreen delineation method involved conducting repeat trials of reproducibility for polygon digitization by selecting five polygons from each year of coverage and digitizing them five times. The resulting distances in any area of difference (i.e., where the digitizations did not align) was measured and averaged. Although Mathew *et al.* (2010) considered Ground Control Point error in their uncertainty calculation for air photos, this value was not used in the total uncertainty calculations as the images were already orthorectified when obtained, and we did not create DEMs from these photos.

Year	Horizontal Positional Accuracy (m)	Onscreen Delineation (m)	Total Uncertainty (m)
1985 (BW)	> 3	0.5	3.5
1994 (BW)	> 3	0.5	3.5
2005 (Coloured)	> 3	0.5	3.5
2009 (Coloured)	> 3	0.3	3.3
2011 (Coloured)	> 1.5	0.3	1.5
2012 (Coloured)	> 1.5	0.3	1.8

Table 3. A breakdown of the total uncertainty calculation of the air photos and digitization that was modified from Mathew *et al.* (2010). The total uncertainty for airphotos is based on the positional accuracy of the air photos and the onscreen delineation (calculated by repeat trials of outlining polygons).

Year	Horizontal Accuracy (m)	Onscreen Delineation (m)	Total Uncertainty (m)
1998	> 0.8	0.3	1.1
2000	> 0.8	0.3	1.1
2007	> 0.75	0.3	1.05
2010	> 0.75	0.3	1.05

Table 4. A breakdown of the total uncertainty calculation of the LiDAR and digitization that was modified from Mathew *et al.*, (2010). The total uncertainty for LiDAR is based on the positional accuracy of the air photos and the onscreen delineation of both depositional and erosional features (calculated by repeat trials of outlining polygons).

2.3.3 Spatial-Temporal Analysis of Moving Polygons (STAMP) model

The STAMP method (Roberson et al. 2007) was used to detect and extract the spatial-temporal patterns of movement and change in blowout erosional and depositional feature polygons. Essentially, the model creates a GIS change layer based on the union of polygons between successive time periods. For the purposes of explanation, T_1 and T_2

represent two consecutive series of digitized polygon layers of the same blowout erosional basin (i.e., a year pairing). The STAMP method determines if there is a union of T_1 and T_2 layers and then creates a change layer ($T_1 \cup T_2$). The spatial-temporal relationships identified are based on overlap (geometric events) and proximity (movement events). The latter are determined by a user-defined distance threshold between polygons in T_1 and T_2 . Resulting events are then classified as change events and their respective areas are quantified (see Tables 5 and 6). STAMP also quantifies the area of polygon expansion in a certain direction, counts events where multiple polygons merge from T_1 to T_2 (i.e., a union event), as well as identifies when a single polygon multiplies from T_1 to T_2 (i.e., a division event).

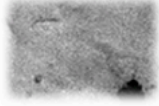
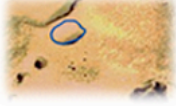




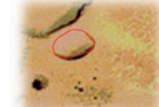








Blowout Geometric Event Name (Epidemiology Event Name)	Description	T1	T2	T1 U T2
Generation	A Generated Polygon in T2 not visible in T1			
Disappearance	A Disappearance of a Polygon from T1 to T2			
Expansion	Area of expansion from T1 to T2			
Contraction	Area of contraction from T1 to T2			
Unchanged (Stable)	Area unchanged			

Table 5. STAMP typology of events to describe geometric changes in polygons based on overlap relations. The red polygons are from T_1 and blue polygons are from T_2 . The second column shows the modified terms that will be used for the purposes of blowout pattern classification. Same classification scheme and method was used for erosional and depositional lobes.

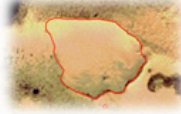


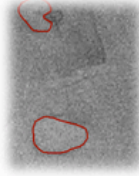
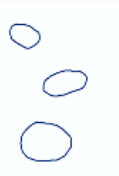







Blowout Movement Event Name (Epidemiology Event Name)	Description	T1	T2	T1 U T2
Clustering (Fragmentation)	T2 within D of T1 expansion or stable			
Divergence by Stabilization (Divergence)	T2 generates within D of T1 Contraction			
Migration and Displacement (Displacement)	T2 within D of T1 Disappearance			
Convergence	T1 disappears within D of T2 Expansion or Stable			

Table 6. STAMP typology of events to describe movement changes in polygons based on proximity relations (a distance threshold set by the user). The red polygons are from T_1 and blue polygons are from T_2 . The second column shows the modified terms that will be used for the purposes of blowout pattern classification. Same classification scheme and method was used for erosional and depositional lobes.

Using the 2012 CCNS aerial photography, 30 erosional blowout features were identified and selected as a subpopulation that would be further analyzed back through time. This subpopulation was selected qualitatively to ensure a representative population of differing sizes, shapes, and stages of evolution. In addition, 10 depositional lobes were selected using the 2010 LiDAR data and also tracked back through time. Only 10 were selected due to the difficulty of accurately defining the limits or boundaries of many depositional lobes in the landscape. These features were digitized by identifying breaks in slope from the DEM. In order to ensure the quality and guide the digitization process for

the depositional lobes, a DGPS was used in the field to trace the outlines of the depositional lobes as precisely as possible. The digitized layers were paired with the neighbouring year layer and run through the STAMP plugin.

2.3.3.1 Geometric events

The STAMP method identifies the following geometric change events: (1) Generation, (2) Disappearance, (3) Expansion, (4) Contraction, and (5) Stable (Robertson *et al.* (2007)). A generation event occurs when a feature is not present in T_1 but appears in T_2 . In terms of blowout morphodynamics, this indicates that blowout initiation has occurred between the two time series. In contrast, a disappearance event occurs when a feature is present in T_1 but does not appear in T_2 , which would indicate that a blowout either disappeared during the incipient phase or stabilized, as has been observed elsewhere. For example, sequential analysis of aerial photography by Jungerius and van der Meulen (1989) showed that many blowouts (17 of 92 identified between 1958 and 1977) along the Netherlands coast near De Blink disappeared shortly after they were formed.

An expansion event occurs when a blowout feature extends and develops between T_1 and T_2 . In certain situations, the size of a blowout exerts form-flow feedback that can either have a positive or negative effect on their development. This can, for example, promote lateral expansion as well as deepening of the deflation basins (e.g., Nordstrom *et al.*, 1990; Hugenholtz and Wolfe, 2006).

Contraction events occur when a polygon feature at T_2 decreases in area within the perimeters defined in T_1 . The area that is no longer considered part of the polygon

feature is classified as a contraction. Blowouts that experience this geometric change could potentially have reached a critical size (length, width, and/or depth) in which erosion and transportation of sand within the deflation basin no longer occurs (e.g., Seppälä, 1984; Hugenholtz and Wolfe, 2006). As such, areas where contraction is occurring could reflect surface stabilization by vegetation, which can lead to the potential closure of the blowout (Gares and Nordstrom, 1995).

Stable events are classified as the area that remains as part of the polygon between T_1 and T_2 . In terms of blowout dynamics, this type of event simply indicates the area of the deflation basin that remains active between the consecutive years, despite whether the blowout is developing or stabilizing. Collectively, these overlapping relationships and events are an important part of understanding the evolution of blowouts, as are the following proximity relationships and movement events.

2.3.3.2 Movement Events

The second set of polygon relationships, classified by Robertson *et al.* (2007) as movement events, include: (1) Displacement, (2) Convergence (3) Fragmentation, (4) Concentration, and (5) Divergence (see Table 6). These events are defined by the STAMP method based on proximity changes between T_1 and T_2 . As such, the movement type is based on a polygon being within a threshold distance defined by the user, which was set at 200 meters for this study as defined by an average distance between blowouts observed in the field and during the digitization process.

A displacement event occurs when a polygon at T_2 is within the distance threshold of a T_1 disappearance polygon. As such, a displacement event could be associated with

blowout migration as they evolve, grow in size, and migrate. This process of migration was observed by Carter et al. (1990) for blowouts in various countries and by González-Villanueva *et al.* (2011) in NW Spain and is a common response in the long-term evolution of blowouts.

Convergence occurs when a polygon at T_1 disappears within the distance threshold of an expansion polygon at T_2 . Such events imply, for example, that a smaller blowout feature has been subsumed by the growth and migration of a larger erosional feature. For example, by comparing the dominant wind direction to the area classified as convergence, it can be determined if development of these blowouts is occurring in the same direction as the dominant wind.

Fragmentation events occur when a new polygon(s) appears at T_2 within the distance threshold of an existing T_1 expansion polygon. In terms of blowout dynamics, this type of movement event can indicate a clustering or amalgamation effect in blowouts where, for example, there is sparse vegetation cover with pockets of active sand surfaces that eventually group into a larger blowout formations.

A concentration event occurs when a polygon disappears between T_1 and T_2 within the distance threshold of a contracting polygon. Such events could indicate blowout stabilization in situations where the deflation basin is decreasing in size and the disappearing portion becomes stabilized by vegetation and deposition (Hugenholtz and Wolfe, 2009; Hesp, 2002).

Divergence occurs when a polygon in T_2 appears within the distance threshold of a contraction polygon in T_1 . This event could potentially indicate that the area where a blowout in T_1 used to be is experiencing stabilization through vegetation encroachment or

reduced localized wind speeds (Hesp, 2002) and that new blowouts are forming within the threshold distance.

2.3.3.3 Modifications to STAMP for geomorphic interpretation

In order to improve the applicability of the STAMP method for analysis of blowout change patterns and morphodynamic evolution, several of the classification events described above were re-named and additional computational refinements were added (as seen in Tables 5 and 6). These include re-naming various geometric and movement events, computing a more relevant change metric that describes the evolution of blowout shape (shape metric), normalization of areal changes to provide rates of change, as well as increasing the directional resolution for quantifying blowout expansion vectors from four to eight cardinal directions.

2.3.3.3.1 Modified geometric and movement events

When classifying polygonal change events it is necessary to consider if the categories appropriately describe the event. Since the STAMP method was developed for use in epidemiology, the category names need to be modified in order to reflect spatial patterns specific to blowouts (Table 5 and 6). For the events that describe geometric changes, generation, disappearance, expansion and contraction are appropriate naming mechanisms for blowouts. The term stable was modified to unchanged, as this area is the deflation basin that has remained from T_1 to T_2 . Select categories for movement events were also modified (Table 6). A displacement event was renamed to migration and displacement, which better describes how active blowouts shift from their original

location. Fragmentation events were re-named clustering events to describe the situation where blowouts develop within some distance threshold of T1. Divergence events were re-named to ‘divergence by stabilization’, which describes the stabilization of a blowout and the concurrent generation of another within the distance threshold.

2.3.3.3.2 Modified change metrics

STAMP also provides a list of change metrics that are simple descriptors of geometric changes of the original polygon layers. Equations behind these metrics are described in Robertson *et al* (2007). Although these metrics provide information on changes within the population, important morphodynamic responses required for interpreting blowout evolution are not described. For instance, normalized rates of areal or volumetric change are a common method of describing morphodynamic process-response relations in dune landscapes (e.g. Carter, 1977; Hesp and Hyde, 1996; Arens, 1997; Hesp, 2002; Hugenholtz *et al.*, 2009; Hugenholtz, 2010; Eamer *et al.* 2013; Eamer and Walker 2013; Walker *et al.* 2013). In this study, rates of areal change for specific events (expansion, contraction, unchanged, and generation) were calculated by dividing the area by the number of years in the series interval. A total rate of areal change was also calculated for each year pair by subtracting the sum of the area of blowouts in T₂ from the sum of the area of blowouts in T₁, then this number was divided by the number of years in the series interval. This provided a quantitative measure of temporal patterns and rates of change.

An additional shape metric was produced to measure and describe changes in the area to perimeter ratio of a blowout. This metric essentially describes if the feature is

becoming more circular (i.e., increasing area:perimeter value) or more complex (i.e., decreasing area:perimeter value) over time. This metric, along with the rates of change, was used to describe morphological changes in blowouts over time for both depositional and erosional subpopulations for all years in each dataset.

2.3.3.3 Modified directional resolution for blowout expansion and/or migration

The STAMP model also characterizes the directional expansion of polygons using a quadrant-based cone model. This model uses a reference polygon centroid (e.g., for T_1) around which a triangle (cone) rotates clockwise from true north in 90° increments within a minimum-bounding box around the union of T_1 and T_2 polygons. The area of the T_2 polygon within each quadrant that has no overlap with T_1 is classified as an expansion in the corresponding direction. From this, a resultant vector that describes the net direction of expansion is generated.

For describing the directional expansion of blowouts and to allow for better comparisons to conventional wind and sand drift roses, the directional resolution for the expansion vector was increased to eight cardinal directions using the same cone-based method. The refinement involves rotations at 45° intervals (vs. 90°) through eight octants, which allows a finer directional resolution. This method was implemented manually in ArcGIS 10.0 and was checked against the directional results from STAMP.

2.4 Results

2.4.1 Erosional Features

Table 7 shows the relevant outputs from STAMP and additional rate calculations for erosional features through time. Geometric type events characterized as expansion, contraction, and unchanged occurred for almost all selected blowouts and year pairings. The generation of blowouts in the subset of 30 features was notably greater from 1985 to 1994 and then began to decrease. Blowout disappearance events were more frequent in later years where there were more union events. As for movement events, clustering and divergence by stabilization were the only two events observed, with the former occurring more frequently and during the earlier years of the sequence.

Year	Number of Blowouts (No. in T1 yr → T2 yr)	Generation	Disappearance	Clustering	Stabilization and Growth	Divergence by Stabilization	Displacement	Contraction Events and Rate (m ² /yr)	Expansion Events and Rate (m ² /yr)	Unchanged Events and Area (m)	Area Change Rate (m ² /yr)
1985-1994	15 → 24	+10	-1	1	0	0	0	-13 (828.78)	+15 (1012.55)	15 (7895.93)	+1646.89
1994-1998	24 → 28	+4	0	1	0	0	0	-21 (1487.22)	+24 (3079.58)	24 (21459.95)	+2011.20
1998-2000	28 → 30	+2	0	1	0	0	0	-28 (945.67)	+28 (4592.24)	28 (33566.29)	+3931.90
2000-2005	30 → 31	+3	-2	1	0	1	0	-29 (1029.29)	+30 (2687.17)	30 (41265.15)	+1672.61
2005-2009	31 → 32	+1	0	0	0	0	0	-31 (1863.31)	+31 (2192.39)	31 (44234.23)	+333.12
2009-2011	32 → 31	0	-1	0	0	0	0	-32 (761.36)	+32 (6647.64)	32 (57955.50)	+4588.52
2011-2012	31 → 30	0	-1	0	0	0	0	-30 (2393.91)	+30 (5122.74)	30 (59802.08)	+2729.48

Table 7. A table that lists the number of blowout erosional features that experienced spatial-temporal (both geometric and movement) events in the neighbouring T1 and T2 year pairings. These values are results from both STAMP and additional manual computation.

Rates of change for these events (Figures 3 and 4) illustrate a different pattern.

The expansion rate increases until 2000, decreases abruptly from 2000 to 2009, increases rapidly in 2009-2011, and decreases slightly again in 2011-2012. Contraction rates follow the opposite pattern of the expansion rates, which is expected due to potential stabilization if there are lower expansion rates and vice versa. The unchanged area

steadily increases as the selected blowouts generally become larger over time. The rate of area change follows the same pattern as the expansion rate.

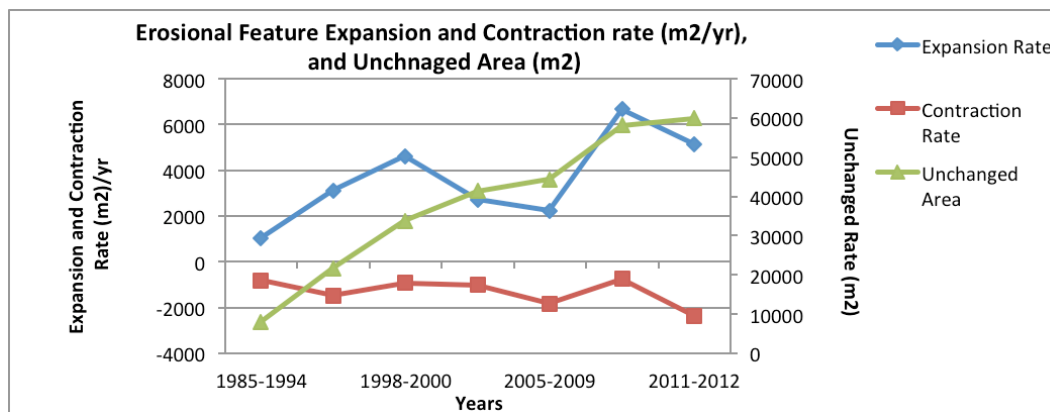


Figure 3. The rate of expansion and contraction (m^2/yr), as well as the unchanged area (m^2) of blowout erosional features. All contraction rate values were given a negative value, as this represents the loss of area in an erosional features. The unchanged area continues to increase over time, showing these features are increasing in size. Expansion rate increases until 2000, quickly decreases from 2000-2009 (with the lowest rate between 2005-2009), and then increases again in the following years. Contraction rate values mirror the expansion rate pattern. These fluctuations in blowout development can be linked to various factors at a landscape scale including increase or decreases in wind speed, precipitation, anthropogenic disturbances, and presence of vegetation.

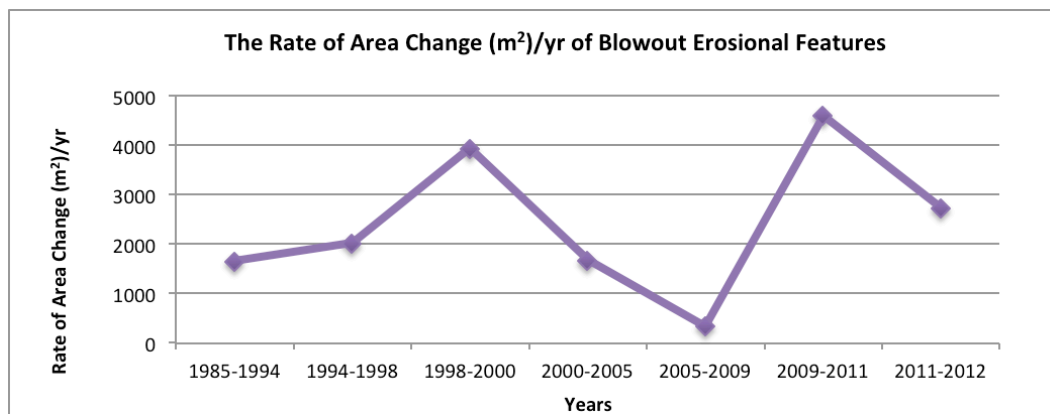


Figure 4. The rate of area change (m^2/yr) within the selected 30 blowout erosional feature subset ($[(\text{T2 area} - \text{T1 area})/\text{number of years between T1 and T2}]$). The rate of area change follows the same pattern as the expansion rate. Variations of these values over time can be linked to various factors at a landscape scale including increases or decreases in wind speed, precipitation, anthropogenic disturbances, and presence of vegetation.

The average shape metric (Figure 5) generally increases for the subset of 15 erosional features, which indicates that the blowouts are becoming more circular over

time (i.e., less complex in shape). Examination individual features' shape metric, as seen in Figure 6, indicates that there are variations in the trends. In addition to an increase in shape metric (more circular) some blowouts are also showing an overall decreasing shape metric (i.e., becoming more complex and less circular), whereas the shape metric of other blowouts increases then decreases and increases again over time. Examples of blowouts on the CCNS landscape experiencing these shape metric patterns are shown in Figure 7.

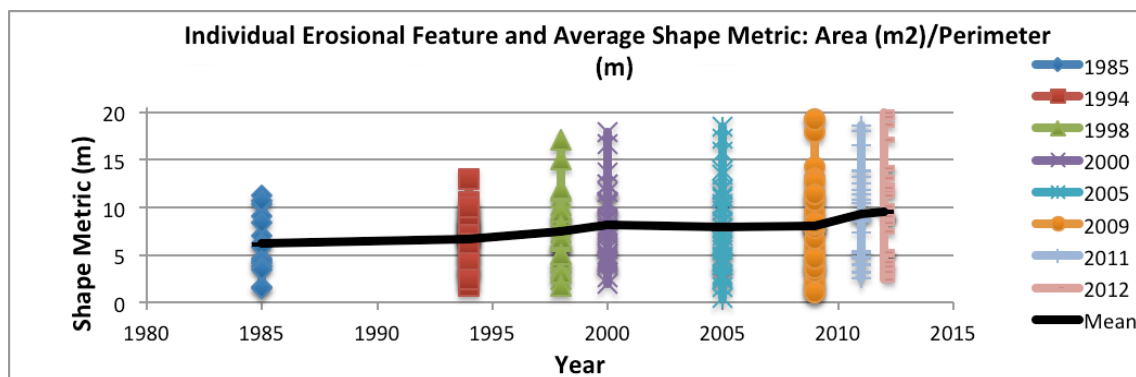


Figure 5. The shape metric values for each erosional blowout feature in a particular year with a line (black) that represents the mean value for each year. The average of the shape metric shows a steady increase in value, which indicates the blowouts are getting larger and more circular/less complex in shape. It is important, however, to examine the shape metric of individual blowouts (see figure 6).

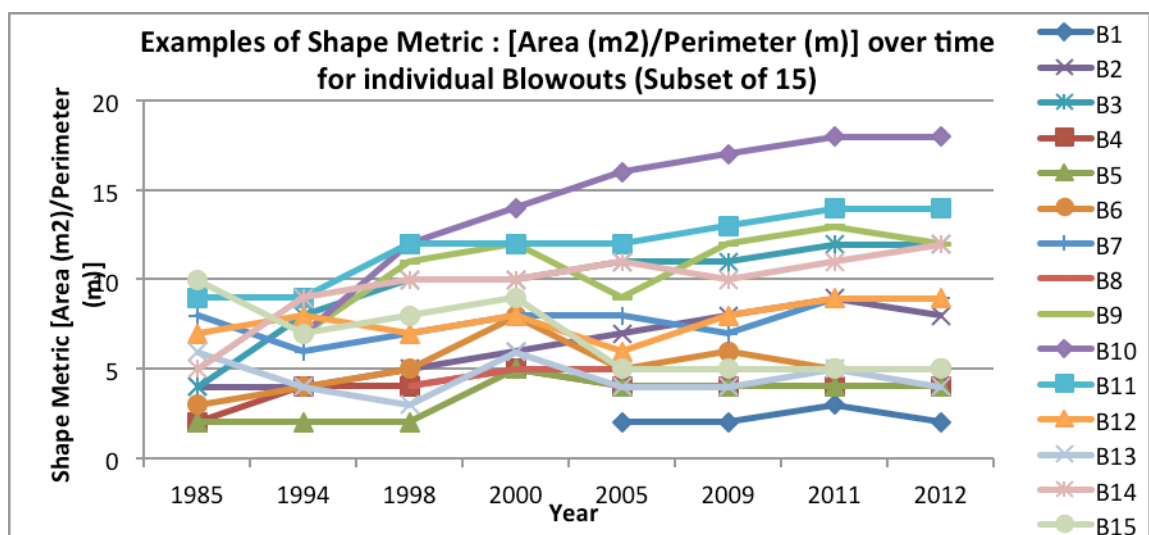


Figure 6. The shape metric values over time for a selected subset of 15 blowouts from the original 30 dataset to discern shape patterns in individual erosional features of the sub-population.

The shape metrics of individual features show that erosional hollows are either: (1) steadily increasing, (2) following the same pattern of the rate of area change (increase, decrease and increase), or (3) have an overall decrease in shape metric (i.e. more complex and less circular).

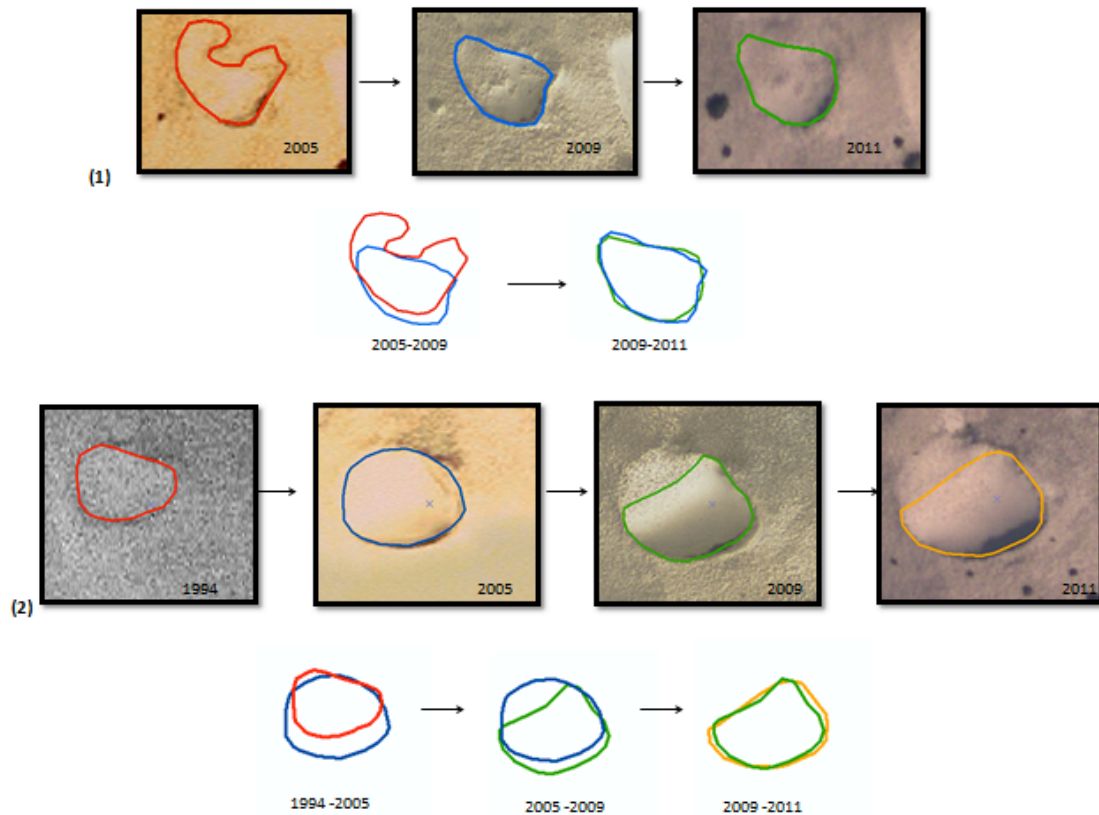


Figure 7. Examples of blowout erosional feature shapes over time as observed by shape metric values and observations during digitization. (a) The erosional feature shape becomes less complicated over time (an increase in area and decrease in perimeter value, which indicates an increase in shape metric over time), which represents an active blowout; (b) The erosional feature shape becomes less complicated and more circular from 1994-2005 (active blowout), then becomes less circular from 2005-2009 (vegetation encroachment), and in 2011 there is an increase in area (removal of vegetation and erosion).

The union and division event patterns detected by STAMP are shown in Figure 8.

Union events occurred more frequently in more recent years of the sequence and only occurred once in the 1985-1994 year pairing. As for division events, only one was

detected in the 1985-1994 pairing. The features that experienced the division event continued to contract or expand over time.

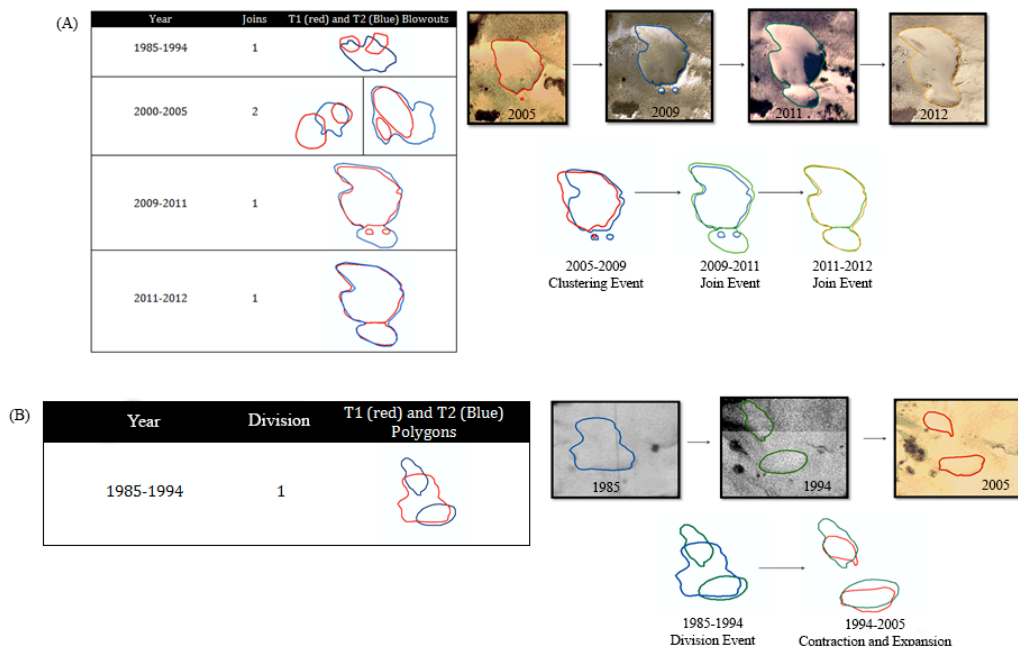


Figure 8. A list of union (blowouts merging) and division (blowouts break into double or multiples) events that occurred in the sequence of airphotos and LiDAR, as well as examples of these events over time. (A) The table on the left is a list of all the union events that occurred in the sequence, and to the right is an example of a union event that occurred as a result of a clustering and expansion events. (B) The table on the left lists the single division event that occurred in the sequence, and to the right is an example of a division event that is followed by contraction events.

2.4.2 Depositional features

The depositional lobe results for STAMP and additional computations are outlined in Table 8. Although the depositional lobes did not change in number over time (i.e., no generation or disappearance events), they show all possible responses (e.g., contraction, expansion, unchanged). The expansion rate and unchanged area decreased between 2000-2007, and then increased in 2007-2010. The contraction rate, however, continues to decrease through the years, but is greater in the first year pairings than

expansion rate (see Figure 9). The area change rate is negative from 1998-2005 and then increases drastically to a positive value in 2005-2010 (see figure 10).

Year	Number of Blowouts (No. in first yr → second yr)	Generation	Disappearance	Contraction Events and Rate (m ² /yr)	Expansion Events and Rate (m ² /yr)	Unchanged Events and Area (m ²)	Area Change Rate (m ² /yr)
1998-2000	10 → 10	0	0	10 (-1315.88)	10 (+671.58)	10 (10381.69)	-745.94
2000-2007	10 → 10	0	0	10 (-1161.66)	10 (+560.65)	10 (6314.46)	-594.11
2007-2010	10 → 10	0	0	10 (-300.40)	10 (+2330.81)	10 (7616.35)	+2030.39

Table 8. A table that lists the blowout depositional features that experienced spatial-temporal (both geometric and movement) events in the corresponding T1 and T2 year pairing. These values are results from both STAMP and additional manual computations.

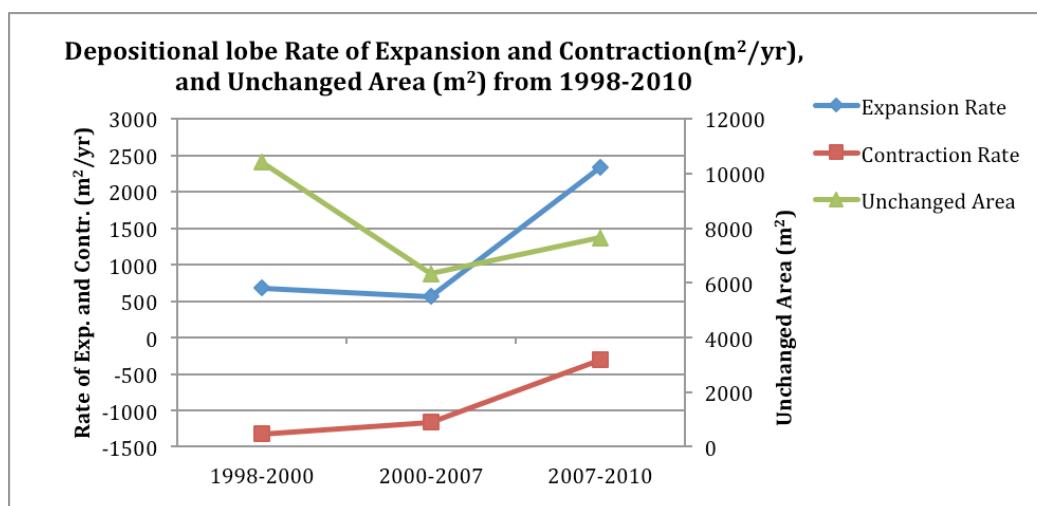


Figure 9. The rate of expansion and contraction (m²/yr), as well as the unchanged area (m²) of blowout depositional features. All contraction rate values were given a negative value, as this represents the loss of area in erosional features. The unchanged area experiences a decrease in 2000-2007 followed by an increase in 2007-2010, which shows that these features experience variability in their shape over time. The expansion rate and contraction rate are again mirrored and show that the rate of development of these features decreased in 2000-2007, but drastically increased from 2007-2010.

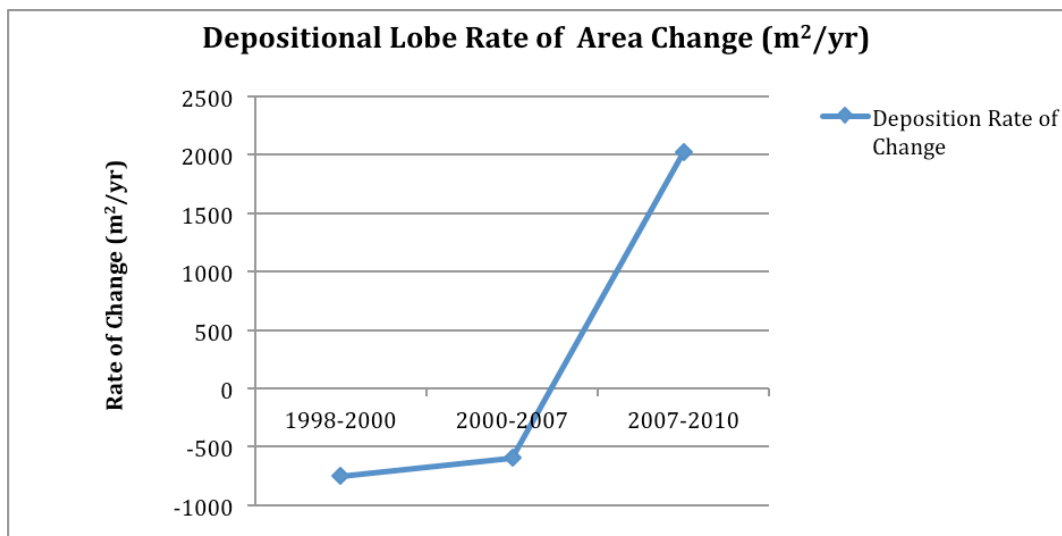


Figure 10. The rate of area change within the selected 10 blowout depositional feature subset ($[(T2 \text{ area} - T1 \text{ area})/\text{number of years between } T1 \text{ and } T2]$). The negative values reveal that the total area of T1 blowouts is greater than the total area of T2 blowouts. These values show that although change in shape may have been occurring, the area of these features did not increase 1998-2007, but from 2007-2010 there was a drastic increase in area change.

The mean shape metric for the depositional lobes steadily decreases from 1998 to 2005 and is followed by a steady increase from 2005 to 2010, as seen in Figure 11.

Changes in the shape metric for a subset of 5 depositional features over time is shown in Figure 12, which indicates that individual depositional features experience a similar pattern as the average seen in Figure 11 (i.e., more circular shape over time). Figure 13 shows an example of this evolution where a depositional lobe has a more complex shape during the initial development stages and then becomes less complex (more circular) as sediment is deposited and the feature expands in all directions.

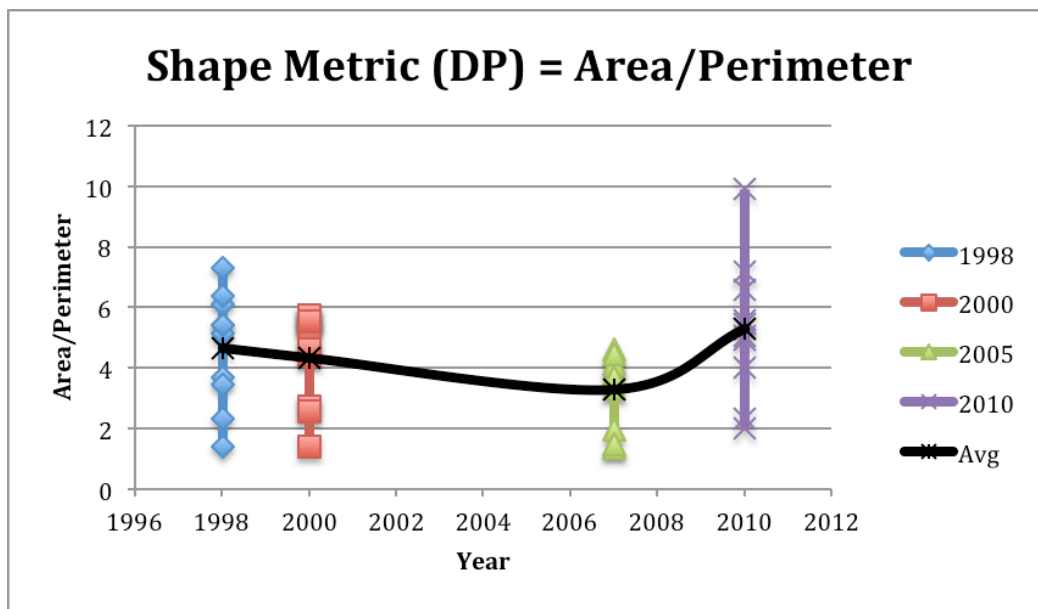


Figure 11. The shape metric values for each blowout depositional feature in a particular year with a line (black) that represents the mean value for each year. The average value indicates that these features become more complex in shape before they expand radially and become more circular.

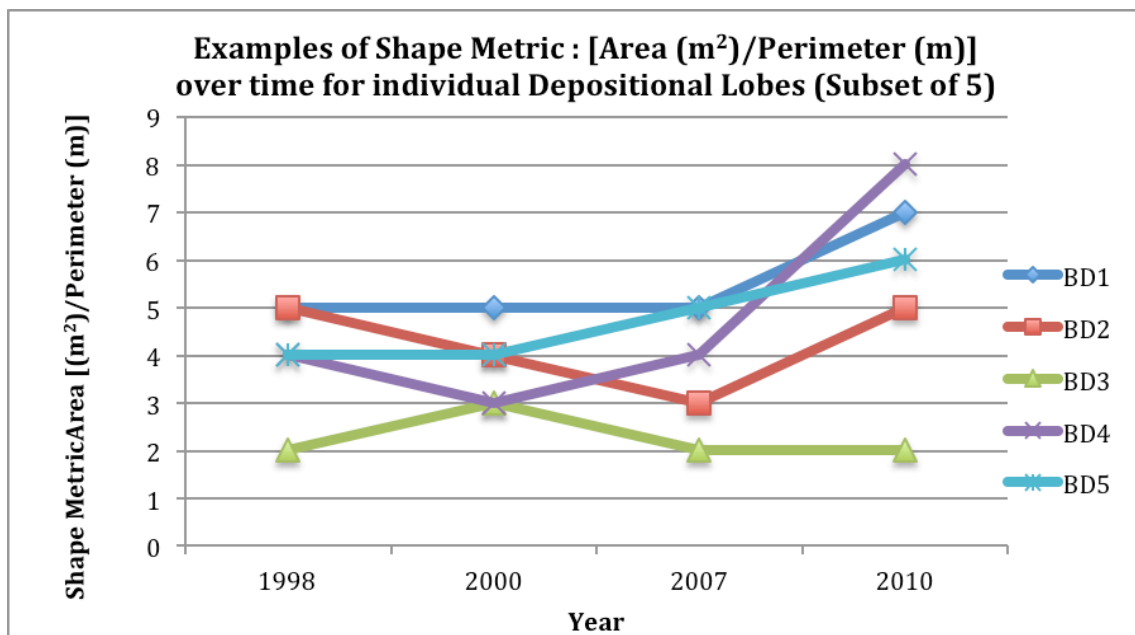


Figure 12. The shape metric values over time for a selected subset of 5 blowout depositional features to discern shape patterns in individual features of the population. These value indicates that these features become more complex in shape before they expand radially and become more circular.



Figure 13. Example of depositional feature shape over time in CCNS. Although the depositional lobes display variety in their morphology over time, the majority of depositional lobes have a similar pattern of evolution; an initial decrease in shape metric followed by an increase in shape metric, which indicates an increase in area and a decrease in perimeter (indicative of a less complicated shape). T1 is outlined and T2 is solid, as well each year has a corresponding colour (1998=red, 2000=blue, 2005=green, and 2010=orange). The black lines represent the area of the blowout hollow.

2.4.3 Directional expansion

The directional expansion of both erosional and depositional features calculated in four cardinal directions (computed by STAMP) and eight cardinal directions (manually computed) are shown in Figures 14 and 15. Resultant vectors for both erosional and depositional features derived from four cardinal directions show the area of expansion is dominantly towards the southeast. Resultant vectors derived from the improved resolution of eight cardinal directions show expansion is dominantly towards ESE for erosional features and SSE for depositional features.

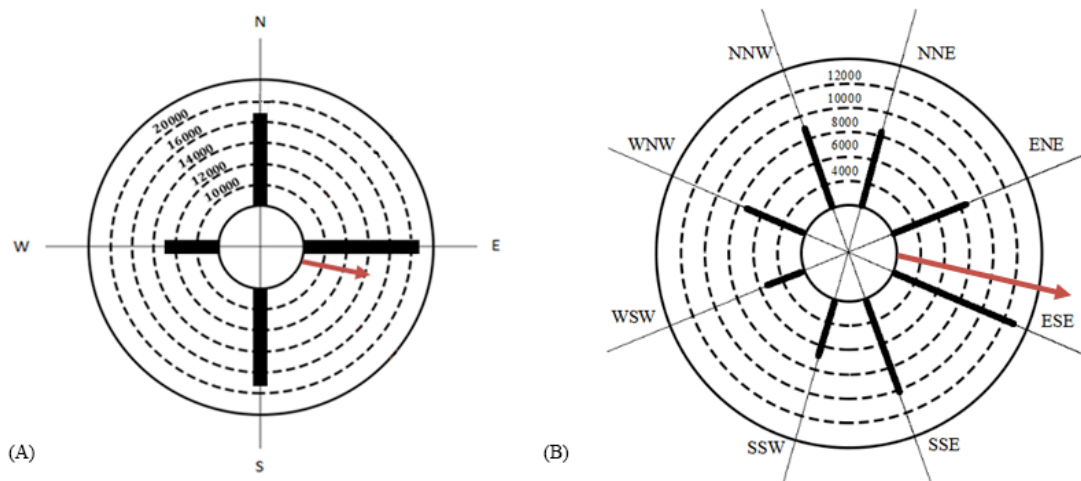


Figure 14. Distribution of the direction of expansion of erosional features from 1985-2012. The length of the black bar corresponds to the sum of the area of expansion in each direction. The red arrow is the resultant direction of expansion. (A) The display of expansion divided into four cardinal directions output by STAMP. (B) The display of expansion divided into eight cardinal directions output manually by computations in ArcGIS. Both roses show that erosional features in CCNS are expanding in the direction of the dominant winds towards ENE, ESE and SSE.

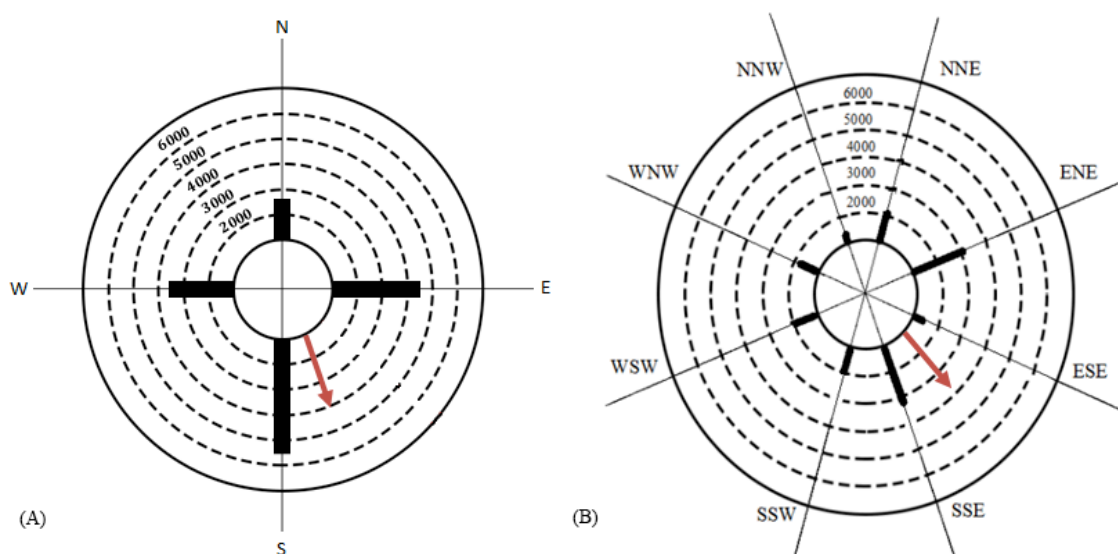


Figure 15. Distribution of the direction of expansion of depositional features from 1998-2010. The length of the black bar corresponds to the sum of the area of expansion in each direction. The red arrow is the resultant direction of expansion. (A) The display of expansion divided into four cardinal directions output by STAMP. (B) The display of expansion divided into eight cardinal directions output manually by computations in ArcGIS. Both roses show that the depositional features in CCNS are expanding in the direction of the dominant winds towards the ENE and SSE.

2.4.4 Resultant sand drift potential (RDP) vectors

The results of the Fryberger and Dean (1979) sediment drift roses are shown in figure 16. The resultant vector for the annual sediment drift rose indicates that the greatest sand transport is occurring towards SSE. Seasonal sand roses for fall, winter, and spring follow a similar trend as the annual sand rose showing greatest sand transport potential towards the SSE for these roses. The summer winds, however, result in minimal movement towards the SSE for these roses. Visual inspection of both the sand and wind roses show that there is a bi-modal and seasonal wind regime in the region, as wind is coming from both the North West and the North East.

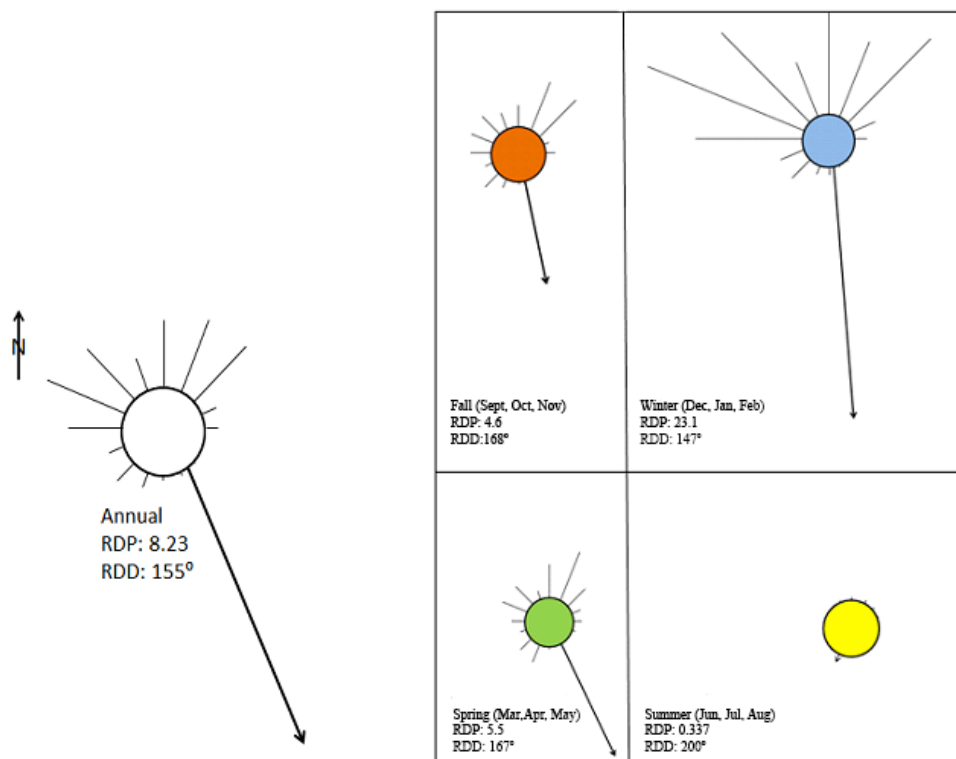


Figure 16. Sediment drift roses created using the Fryberger and Dean (1979) method. (A) An annual sediment drift rose with the resultant indicating sand being dominantly transported towards the SSE (155°) (B) Seasonal sediment drift roses indicating that in Fall, Winter and Spring the dominant direction of sediment transport is towards the SSE and in Summer is towards the SSW.

2.5 Discussion

As demonstrated in the STAMP results, the blowouts of CCNS exhibit common morphodynamic responses and patterns of change. As observed from a regional scale there are two common morphodynamic responses: features become more circular over time (both erosional and depositional), and blowouts develop towards the direction of the dominant wind regime. There are also five patterns of change that are identified: generation, expansion and contraction, stabilization, re-activation, and division and union. From these responses and patterns a model of evolution for blowouts of CCNS is presented. As well, the contribution of spatial-temporal polygon analysis for the study of blowouts and dune features at a landscape scale and future work are explored.

2.5.1 Directional Expansion of Blowouts in CCNS

The dominant winds can be seen in the wind roses in Figure 1, the direction of expansion roses created from STAMP and manual computations are in figures 14 and 15, and the Fryberger and Dean (1979) sediment drift roses are in figure 16. All of these figures define the dominant wind, sand transport and expansion of blowouts to be towards the South South East, East South East and East North East, and that the dominant winds are coming from the North West and North East in the CCNS dune fields. As found by Jungerius *et al.* (1991), a shift in dominant wind direction can alter the shape of the features. When the blowout initially develops, deposition occurs in all directions radially and results in a more complex shape. As the blowout continues to develop the multidirectional wind regime in CCNS is potentially the reason both erosional and depositional features expand radially and are becoming more circular over time. This

may explain why saucer and bowl blowouts are more common in this landscape (as observed in air photos and in the field).

The use of all three roses (sediment transport, wind and STAMP) provides greater validity to the results. As well, the results link process from the sediment transport roses and response from the STAMP roses. As stated by Pearce and Walker (2005), the Fryberger and Dean model has frequency and magnitude biases, which limits the use of the technique in some regions and/or studies. By combining the three methods of determining the direction of blowout expansion, a more holistic view is gained on wind patterns, sediment transport, and expansion of blowout features.

2.5.2 Observed Morphological Stages for Blowouts in CCNS

2.5.2.1 Blowout Generation

The generation of a blowout occurs when there is an initial disturbance of the bare sediment deposit (minimal vegetation cover) that results in a notch, also referred to as an incipient blowout (Gares and Nordstrom, 1995; Hesp, 2002). As observed from the STAMP results at a decadal scale, the blowout continues to develop beyond generation when expansion persists to be greater than contraction. The presence of vegetation is one of the most important factors in the initiation and development of blowouts, as it is a limiting control of aeolian activity (Jungerius and van der Meulen, 1988; Saunders and Davidson-Arnott, 1990; Gares and Nordstrom, 1995; Hesp, 2002; Dech et al., 2005; Den Van Ancker et al., 2006; Hugenholtz and Wolfe, 2006; Hugenholtz and Wolfe, 2009). The aerial photos in 1985 were taken in March and the planting occurred in April. Therefore, there is a time period where blowouts could have initiated and developed in areas of sparse vegetation. As observed by the NPS historian involved in the vegetation

planting campaign, not all vegetation populations survived and some areas experienced vegetation die-back and/or failed to thrive, which could have left areas of sand exposed to aeolian erosion and the potential to initiate blowouts (Burke, 2012). The greatest generation of blowouts occurred between 1985 and 1994, which is hypothesized to be linked to the planting of vegetation. In this period predominantly beach grass (*Ammophila breviligulata*), and other species such as Austrian Pine (*Pinus nigra*), Japanese black pine (*Pinus thunbergii*), Bayberry (*Myrica pensylvanica*) planted by National Parks Services staff and volunteers in efforts to stabilize approximately 934 acres of the Provincelands dunefields (the areas of revegetation has been outlined in Figure 2) (Madore and Leatherman, 1981).

2.5.2.2 Blowout Development via Expansion and/or Contraction

A blowout develops when the area of expansion is greater than contraction, which is required to maintain the erosional form. However, the results from the shape metric show that the development of CCNS blowouts is not linear. Although the average shape metric shows a steady increase over time, indicating that blowouts are becoming larger and more circular in shape, the shape metric for individual blowouts within the subpopulation is variable. Therefore, during development blowouts experience both expansion and contraction responses at various times in their evolution, sometimes simultaneously (see Table 5). The geometric events that occurred most for both erosional and depositional features was contraction and expansion, as seen in Figures 7 and 8. Fluctuations in blowout development in CCNS (expansion and contraction) can be linked

to various factors at a landscape scale including increase or decreases in wind speed, precipitation, anthropogenic disturbances, and presence of vegetation (Hesp, 2002).

2.5.2.3 Blowout Union or Division

The results for the union (when several blowouts expand into one larger feature) and division (one larger feature splits into smaller features that continue to evolve) derived by STAMP provide insight to the manner and speed at which blowouts can expand or contract. The only division event within the sequence occurred between 1985 and 1994. This is potentially linked to re-vegetation initiatives within CCNS, which may have stabilized and divided the initial blowout into two smaller individual blowouts. There were also several union events that occurred throughout the sequence, however, the occurrences were concentrated towards later years and were usually preceded by clustering, generation, and/or expansion events. Furthermore, the union of blowouts resulted in the acceleration of blowout development. For example, figure 8A, shows the expansion of 3 blowouts into one large blowout within three years and greatly expand the area of the blowout.

Jungerius *et al.* (1991) found that the effects of high-magnitude wind events on aeolian features are of minor importance compared to events with lower magnitude and high frequency. However, in CCNS, as seen by union events, the expansion of features can occur at a relatively fast pace and within a shorter period of time, potentially within one high wind event. Using the blowout in figure 8 (A) as an example, from 2009 to 2011 the three blowouts expanded and merged into two larger blowouts that shared an erosional wall. Then between 2011 and 2012 the erosional wall was blown out so that the

blowouts became one larger feature. In addition, nine of 32 blowouts have experienced a union event, therefore, indicating that the union is a re-occurring pattern of change that is contributing to the evolution and rapid rate of expansion in CCNS.

2.5.2.4 Blowout Stabilization

Blowout stabilization occurs where contraction has become much greater than expansion and the feature eventually becomes inactive. During this phase, sediment deposition and/or vegetation stabilization occur in the erosional basin. Gares and Nordstrom (1995) referred to these regions as ‘stagnation zones’. Within CCNS, many blowouts that showed a consistent decrease in shape metric also experienced stabilization. During this process, the area of the erosional feature decreased and the perimeter increased with irregular vegetation encroachment, as seen until 2009 in Figure 7 (b). There are many factors that influence the closure or stabilization of blowouts, including the availability of sediment supply outside of the blowout, vegetation colonization, climatic variability (e.g. increased precipitation, lower winds), and/or land use change/disturbance (Gares and Nordstrom, 1995; Hugenholtz and Wolfe, 2006; Hesp and Walker, 2013). These are all potential factors at CCNS, however, the most evident is vegetation encroachment as observed from the air photos (e.g. Figure 7 (b)).

2.5.2.5 Blowout Re-activation

The re-activation of a blowout occurs following a disturbance to a previously stabilized (vegetated) surface resulting in increased aeolian activity. Barchyn and Hugenholtz (2013) explain that dune re-activation can occur through (1) sediment erosion, (2) sediment deposition, and (3) direct disturbance (e.g., high winds, destructive

land use changes, fire, aridity, biogenic or human disturbance, or some combination). The authors also suggested that blowouts could represent incipient reactivation features within a larger dune field system. In their four-stage blowout evolution model, Gares and Nordstrom (1995) explained that there are potential factors that can truncate the model: (1) changes in feedback between landform, wind regime, and vegetation cover, (2) variations in the wave climate associated with foredune erosion events, or (3) human intervention. Thus, there are a variety of factors that span spatial and temporal scales and related land cover or land use changes that may result in a stabilized blowout becoming re-activated. As such, there is research that explores linkages between blowouts and re-activation; however, it has not yet been acknowledged that re-activation is a stage in the broader morphodynamic evolution of blowouts.

Although re-activation did not occur in the 30 selected blowouts, it was observed in the air photo sequence and during field surveys in CCNS (May and October 2012, and October 2013) that previously stabilized surfaces can become exposed to wind erosion. Figure 7 shows an example of a blowout that experiences vegetation encroachment (decreases in size) followed by expands in following years. Although this is not an example of complete stabilization of a blowout followed by re-activation, this example shows that blowouts in CCNS tend to experience partial stabilization by vegetation encroachment, followed by a removal of vegetation and expansion of the blowout. Furthermore, STAMP is capable of detecting re-activation through the detection of disappearance and generation of a blowout in the same location.

2.5.3 Blowout Evolutionary Model

The spatial-temporal pattern analyzes in this paper suggest that blowouts in CCNS are developing in a series of stages: (1) generation; (2) contraction and expansion; (3) union or division; (4) stabilization; and (5) re-activation. As stated by Hesp (2002), blowouts will generate or initiate in response to: (1) wave erosion along the seaward face of a foredune; (2) topographic acceleration of airflow over the dune crest; (3) variability in climate; (4) vegetation removal or burial; (5) water erosion; (6) high velocity wind erosion; or (7) anthropogenic disturbances. Once in an incipient stage, the blowout will expand and contract in the direction of the dominant winds present at the time. As mentioned, the wind regime in CCNS is multi-directional and results in both the erosional and depositional features expanding radially. In response, if there is no interference (e.g., large bushes or trees) blowouts tend to become more circular over time. As these features become larger by expansion and cluster in an area, there is potential for the union of blowouts. At this point it is also possible that blowouts experience stabilization, which is common in CCNS by vegetation encroachment and can potentially divide larger blowouts into multiple smaller features, or simply decrease the size of individual intact blowouts. At any point a stabilized blowout can experience a disturbance to the stabilizing surface and re-activate, which begins the cycle of development again.

This model of blowout development in CCNS roughly follows a modification of Gares and Nordstrom's (1995) cyclic evolution model, which involves the interactions of changing landforms, wind regimes, and vegetation removal or regrowth. The four stages of their model include: (1) notching and initiation, (2) incipient blowout, (3) full blowout, (4) and closure by foredune formation across the throat. However, our research

presents two new evolutionary stages, and one stage modification to the Gares and Nordstrom (1995) model. First, is the potential union or division event that can occur between steps three and four, as explained above. Second is the re-activation stage, which can occur after the closure or stabilization of a blowout. Although, Gares and Nordstrom (1995) did make mention of potential factors that could truncate the model, they did not include re-activation as a potential step in the evolution of blowouts. In the case of CCNS, closure of blowouts or stabilization does not occur as a result of foredune formation across the throat as explained by Nordstrom and Gares. Most blowouts in CCNS are not in the foredune and closure occurs due to vegetation colonization around the margins or within the blowout basin. This modified model presents a more complete description of the evolution of blowouts in CCNS from spatial-temporal pattern analysis.

2.5.4 Utility of the STAMP method

The STAMP method provides spatial-temporal information of geometric events, movement patterns, area changes, directional change, and union and division of polygons features (blowouts). With additional computations of change metrics and area changes, the results provide an overall profile of the feature population and change through time. As noted by Hugenholtz *et al.* (2013), there has recently been a shift from single dune studies to dunefield scale studies (as studied in this paper for the blowouts of CCNS) that also incorporate spatial analysis to understand patterns of change, activity, conditions, and relations (e.g. Tsoar and Blumberg, 2002; Hugenholtz and Barchyn, 2010; Ewing and Kocurek., 2006; Ewing and Kocurek., 2010; Kocurek and Ewing, 2005; Dech *et al.*, 2005; Mathew *et al.*, 2010). Therefore, STAMP and the modifications to the technique in this paper provide results that are applicable to the studies of various features and

landscapes, and render the process of producing results less time consuming for larger data sets. For example, the computations of dune migration rates studied by Bailey and Bristow (2004), which were calculated for three years, could have been automated and computed for more than three years of air photos. Another example of a study where STAMP could have automated computations would be the study of population characteristics, area change, and merging of Barchan dunes by Bourke (2010). STAMP could also add another dimension to the results by classifying change into geometric and movement events and providing information on the direction of expansion. Therefore, STAMP is an automated, systematic and highly useful method for researching the spatial-temporal patterns of change in various coastal features at a local and a landscape scale.

2.5.5 Future Work

In addition to STAMP, when performing 2D analysis of change on geomorphic features it is important to consider that there are additional computations to include. It is interesting to couple results of STAMP with Fryberger and Dean (1979) sediment drift roses and wind roses to compare directional results, as done in this paper. An analysis of volumetric change (3D analysis) using LiDAR data is an important calculation to include; especially for features such as blowouts that have erosional hollows and depositional lobes where sand can be scoured or accumulate while no change is made to the feature boundaries. In addition, further overview of land use change reports (park or management reports) can be used to understand human impact in relation to the results of change provided by STAMP. Also, a supervised classification of air photos series can be run to assess changes in vegetation and bare sand cover. This can provide information if the landscape is dominated by stabilizing vegetation species, re-activating by removal of

vegetation, or activating with dominantly bare sand surfaces. These methods coupled with STAMP computations allow for explanations of spatial-temporal results at a landscape scale.

2.6 Conclusion

The quantitative analysis of spatial-temporal characteristics and patterns of blowout populations in CCNS at a landscape scale is examined using STAMP and the modifications. This method gives us information on population numbers over time, classifies and computes the area of geometric and movement events for each year pair, the area of expansion by cardinal direction, classification of feature union and division events, as well as a shape metric to describe blowout morphology over time.

The results from STAMP and additional computations on the blowouts of CCNS provide the following information on the evolution of these features: (1) both geometric events and movement events occur for blowouts in this landscape as they develop; (2) the generation of blowouts in CCNS is greatest in 1985, which by reviewing NPS reports, is potentially related to a coupling of intense vegetation planting campaigns followed by vegetation-dieback (leaving local, sparsely vegetated surfaces); (3) from the three roses (wind, sediment transport, and STAMP) it is evident that these features are expanding and sediment is being transported towards the dominant winds from the North West and the South West; (5) the shape metric shows that the erosional and depositional features are generally becoming more circular as they develop, which is potentially a result of the multidirectional wind regime; (6) the evolution of these features follow a similar pattern to that described by Gares and Nordstrom's Cyclic Blowouts Evolution Model with two

additional stages and one stage modification: union and division events can occur as the features expand and stabilize, as well re-activation events can occur when there is an initiating factor present (e.g. strong winds, storm event, human disturbance, vegetation die-back, etc.).

When using the STAMP method, one should consider: (1) STAMP is a two dimensional analysis of features on a landscape, which allows the potential to further investigate change using three dimensional data types such as LiDAR to examine the volumetric changes over time; (2) land use change and human activity can be used to explain and understand change seen in STAMP results by consulting NPS staff or researching NPS historical reports; (3) by creating a sediment transport rose, annual and seasonal wind roses, and a directional expansion STAMP rose, process and response are linked and better understood; (4) the main benefit to using STAMP is that it is an automated method to evaluate populations of features (polygons), such as blowouts, at a landscape scale, which simplifies computation.

3.0 Spatial-temporal and Volumetric Analysis of Blowouts in Cape Cod National Seashore, Massachusetts, USA

3.1 Introduction

Blowouts are depressions, hollows, and/or troughs that form in pre-existing sand deposits by aeolian erosion (Carter *et al.*, 1990; Byrne 1997; Hesp and Hyde, 1996; Hesp and Pringle, 2001; Hesp, 2002; Hugenholtz and Wolfe, 2006; Hesp and Walker, 2012, Smyth *et al.* 2013). Although common features in desert and coastal dune landscapes and important indicators of climatic and other landscape changes (Hesp and Hyde 1996; Hesp, 2002, Smyth, 2012), there are relatively few detailed studies on blowout development, morphodynamics, and/or longer-term evolution to date (e.g., Abhar *et al.*, 2014, in review; Hesp and Hyde, 1996; Hesp, 2002; Hugenholtz and Wolfe, 2006; Hesp, 2011; Smyth *et al.*, 2012, 2013). Blowouts are generally categorized by their morphology, which varies from saucer, cup/bowl, or trough shaped and other forms that have both erosional and depositional features (Gares and Nordstrom, 1995; Hesp, 2002). The development of blowouts is both facilitated and limited by factors such as dominant wind speed and direction, the presence or absence of vegetation, climatic variability, sand supply, topographic effects on flow dynamics (e.g., flow constriction and/or acceleration), water and wave erosion, and anthropogenic changes within a landscape (e.g. Pluis, 1992; Gares and Nordstrom, 1995; Hesp 2002; Smyth *et al.*, 2012, 2013; Barchyn and Hugenholtz, 2013). Overall, the main driving force controlling blowout size, shape, and direction of expansion is the wind regime and resulting complex flow dynamics within blowouts that promote and maintain erosion (e.g., Landsberg, 1956; Cooper, 1958; Jungerius *et al.*, 1981; Gares and Nordstrom, 1995; Hesp, 2002; Hesp and

Pringle, 2001; Smyth *et al.*, 2012, 2013; Hesp and Walker, 2013). Vegetation is another critical factor in blowout initiation, as the presence of vegetation assists in the formation of the feature, and. In some cases, dense and/or thickly or deeply rooted marginal vegetation may restrict or alter blowout expansion or development. Vegetation removal or failure to thrive allows for the erosion of active sands and for initiation and/or further development of blowout erosional features (Melton, 1940; Carter *et al.*, 1990; Hesp, 2002; Barchyn and Hugenholtz, 2013).

Recently, airborne light detection and ranging (LiDAR) has been used to map and analyze detailed surface changes in coastal dune environments, including blowouts (Smyth *et al.* 2011; Smyth *et al.*, 2012; Abhar *et al.*, 2014, in review), to provide estimates of volumetric and morphological change over time (e.g. Woolard and Colby, 2002; Brock *et al.*, 2002; Sallenger *et al.*, 2003; Houser and Hamilton, 2009; Eamer and Walker, 2010; Eamer and Walker, 2013; Darke *et al.* 2013) As such, analysis of repeat Digital Elevation Models (DEMs) and/or blowout erosional or depositional feature polygons, allow for multi-temporal investigation of spatial patterns in blowout areas that provides new insight into inter-annual to decadal scale morphodynamics and evolution.

This paper explores the volumetric and areal expansion of blowout dunes in Cape Cod National Seashore (CCNS) using airborne LiDAR and recently developed geomorphic change detection methods (Wheaton *et al.*, 2010). The study identifies a sub-population of blowouts in CCNS for which repeat aerial LiDAR surveys are available dating back 15 years. Volumetric and areal changes for this sub-population of blowouts, including both erosional basins and depositional lobes, are quantified and tracked through

time to interpret their morphodynamics and sediment budget responses. Specific research objectives include: (1) to calculate statistically significant volumetric and areal changes in a select sub-population ($n=10$) of blowouts in CCNS using available airborne LiDAR from 1998, 2000, 2007, and 2010, (2) to quantify changes in surface cover (vegetation and active sand) over time by a supervised classification method using aerial photography from 1985, 1994, 2001, 2005, and 2009, (3) to estimate the competence of the regional wind regime over the observation period (1998-2010) as a proxy measure for aeolian activity, and (4) to combine these results to interpret inter-annual to decadal-scale morphodynamics and evolution of blowout features within CCNS.

3.2 Study Area

CCNS is a protected area managed by the U.S. National Parks Service (NPS) that encompasses 176 km² of beach and upland landscapes on Cape Cod, Massachusetts, USA (Figure 17). CCNS hosts one of the highest densities of saucer and bowl blowouts in the world based on an analysis of Google Earth photography by one of the authors (Hesp). These dunes have been exposed to both anthropogenic disturbance and reclamation (e.g., replanting and stabilization efforts) over the years. Currently, the vegetated areas of the landscape are dominated by American beach grass (*Ammophila breviligulata*), which is an effective agent in controlling the vertical accretion and horizontal movement of coastal dunes and blowouts (e.g., Maun, 1998; Maun and Perumal, 1999), and is spanning approximately 1800 ha of the CCNS (Timm *et al.*, *in review*).

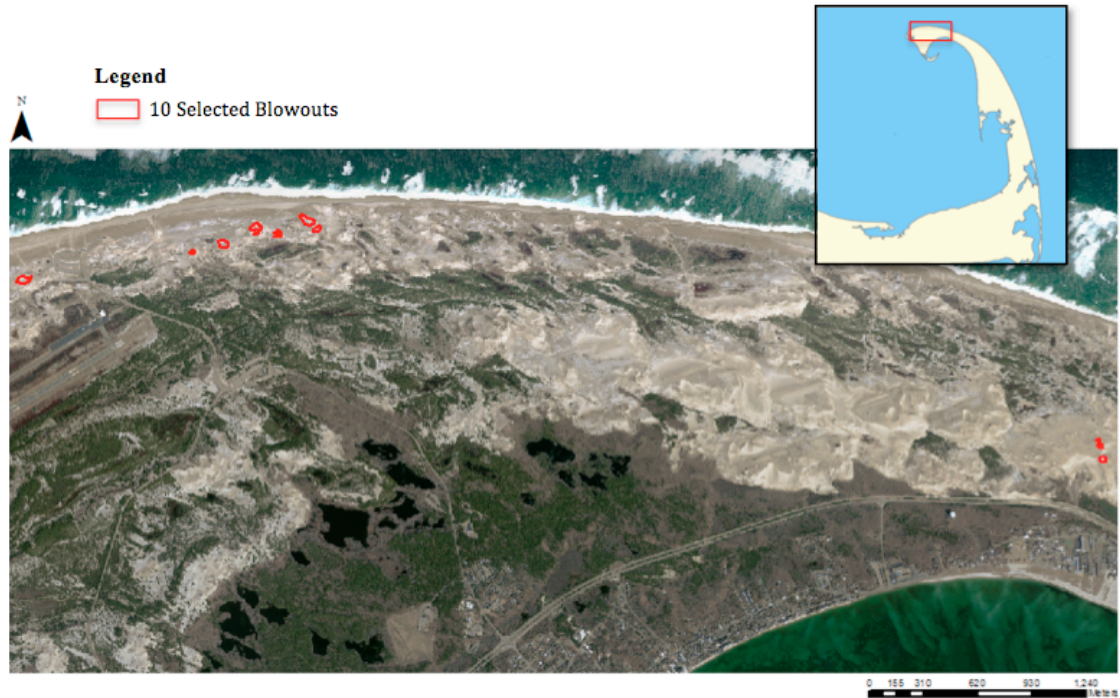


Figure 17. An aerial image from 2009 with a view of the proposed area of study of blowouts in Cape Cod National Seashore, Massachusetts measuring approximately 35 km². Ten blowouts were selected and digitized to analyze volumetric and aerial changes.

Regional climate and wind patterns are also dominant driving forces in the morphodynamics of dune systems in CCNS. This region is also affected by mature Atlantic hurricanes, often calmed to tropical storms, that have been previously formed in the lower latitudes and move north-west. The hurricanes that have the greatest winds and impact on the landscape are those that travel northward over the warm waters of the Gulf Stream (as hurricanes derive their energy from the oceans warm waters) and move past New England. Although the winds and intensity of many hurricanes weaken during the journey to the Cape Cod region, sustained winds of 20 - 35 m s⁻¹ are not uncommon (Simpson and Riehl, 1981; Boose *et al.*, 2001).

The Provincelands dunefield is a prominent and geomorphically distinct region within the CCNS and landscape, covering approximately 35 km² (Figure 1). Forman *et*

al. (2008) note that there are at least eleven discrete parabolic dunes with distinct arms and depositional lobes in this landscape and most of these are being reworked to various degrees by contemporary blowout development. Given the diversity of blowout features with varying shapes, sizes, and stages of development, coupled with the broader landscape, land use variability, and plentiful record of aerial photography and LiDAR, the CCNS region presents a prime study area for analysis of blowout development and volumetric analysis.

3.3 Data and Methods

3.3.1 Data Sources and Pre-processing

LiDAR data was obtained from the National Oceanic and Atmospheric Administration online data access viewer (NOAA Coastal Services Center, 2014), and the orthorectified air photos were obtained from NPS-CCNS staff and the State of Massachusetts Office of Geographic Information (MassGIS) (Massachusetts Office of Geographic Information, 2013). The orthophotography used in this analysis dates back to 1985, as listed in Table 9, and the LiDAR data was available back to 1998 (Table 10). Both datasets were assessed for their post-processed quality for identifying and assessing blowouts in CCNS by reviewing their positional accuracy between years, as well as horizontal accuracy of the LiDAR data.

Year	Source	Horizontal Accuracy	Scale	Pixel Resolution
1985 (BW)	USDA	> 3 m	1:60,000	1 m
1994 (BW)	MassGIS	> 3 m	1:10,000	0.5 m
2001 (Coloured)	MassGIS	> 3 m	1:5,000	0.5 m
2005 (Coloured)	MassGIS	> 3 m	1:5,000	0.5 m
2009 (Coloured)	MassGIS	> 3 m	1:5,000	0.3 m

Table 9. A list of the source, accuracy, scale, resolution and extent of the orthorectified air photos used in this study to digitize the blowout erosional features.

Year	Horizontal Accuracy (cm)	Vertical Accuracy (cm)	Point Spacing (m)	Residual Z (mm)	Extent
1998	> 80	> 15	1	2.2	Entire Provincelands
2000	>80	> 15	1	1.5	Entire Provincelands
2007	>75	> 20	1	3.8	Entire Provincelands
2010	>75	> 20	1	0.5	Entire Provincelands

Table 10. A list of the source, horizontal and vertical accuracy, resolution and extent of the LiDAR (obtained from NOAA Coastal Services Center) used in this study to calculate volumetric change of the selected ten blowout erosional and depositional features in CCNS.

Digital Elevation Models (DEMs) were created from the ground LiDAR points using a Kriging model to interpolate the points in a 3D mapping software, Surfer 12. The chosen interpolated grid size was 1 meter, as this value is equal to the nominal spacing of all surfaces used. As well, 1 meter is suggested to be a sufficient grid size to capture morphological and volumetric changes of coastal dune systems (Woolard and Colby, 2002; Eamer and Walker, 2010). The model performance (for the 1 meter gridding) was assessed in Surfer by running a cross-validation for each surface. This calculates the difference between the surface points and the interpolated points, which is called a residual z. The cross-validation process removes a data point from the data set before an

interpolative 1 meter surface model is created on the remaining data points. Then the difference between the previously removed measured point and the modeled points are calculated to give the residual z value (see Table 10). The 1 meter grids were then clipped to create an individual DEM for each blowout (including both erosional and depositional features) in each year.

Wind data (hourly wind speed and direction) were obtained from NOAA's National Climatic Data Center (NCDC) for 1998 to 2010 (National Climatic Data Center, 2013) from Provincetown Municipal Airport (42.072°, -70.2011°) within CCNS. The percentage of winds that were above the threshold velocity of 9.6 m s^{-1} (calculated using Bagnold's (1941) equation for the mean grain size of sands in the study area) was calculated for each year to compare against volumetric changes. Since there were no data recorded during Hurricanes Bonnie (on August 24th, 1998) and Noel (on November 3rd 2007), a daily comparison was calculated between the Provincetown and Hyannis Wind stations to find the difference in hourly wind speeds in both years. It was found that the average difference was $+2.1 \text{ m s}^{-1}$ in 1998 and 1.7 m s^{-1} in 2007. The plotted values for Provincetown and Hyannis wind data also follow the same patterns, with Provincetown consistently having higher winds. Therefore, the Hyannis data was used to fill the data gap in the Provincetown wind data record for this day, with an addition of 2.1 and 1.7 m s^{-1} to the values in respective years.

3.3.2 Volumetric Change Estimates

DEMs were imported to the Geomorphic Change Detection (GCD) software package developed by Wheaton *et al.* (2010) to calculate statistically significant

volumetric changes for each of the LiDAR survey intervals (Table. 2). A user-defined threshold of 20 cm that corresponded with the largest vertical accuracy value across the years of LiDAR surveys was used to detect volumetric changes at a 95% confidence level. The output is a difference of DEM (DoD) surface, which only include cells with probability above the confidence interval in the volumetric sediment budget estimate from the DoD. DoD surfaces were created for all LiDAR year pairings and each of the selected ten blowout features. GCD output values for the volume of both erosion and deposition, which was further normalized for time in order to display rates of volume change in individual features.

3.3.3 Area Change Calculations

The change in area of the erosional features was also calculated by first manually digitizing each blowout in the subpopulation in each year in ArcGIS 10.0. To derive the area of expansion, the areas of individual polygons were calculated in the attribute table and subtracted from the area of the same feature from the previous year. There are methods that can be used to automate this calculation such as Spatial-Temporal Analysis of Moving Polygons (STAMP) (Robertson *et al.* 2007; Abhar *et al.*, 2014, in review), however, since there were only ten features, it was quicker to calculate using ArcGIS tools and manual calculations. Once area expansion values were obtained, a volume to area ratio was also calculated in order to compare two and three-dimensional changes for individual blowouts.

3.3.4 Supervised Classification

To classify land cover changes (vegetation and active sand cover) of the Provincelands dunefield the remote sensing program Environment for Visualizing Images (ENVI 4.2) was used to run maximum likelihood supervised classifications on mosaics of all years of the air photo series. Before the imagery was classified the series' went through two pre-processing routines. Since the 1985 air photos were black and white imagery, a synthetic RGB colour image was created in ENVI 4.2. This changes the greyscale image into a colour image by applying high pass and low pass filters to the image, which separates high and low frequency information. The hue, saturation, and value data are then transformed into red, green, and blue (RGB) space. The second pre-processing routine was the masking of the pixel values that represented water. Since water contained the same reflectance values of other surface features that are of interest, these pixels could potentially skew the classification results by false classifying the water class as another surface class. Therefore, using the mask builder in ENVI 4.2, a binary image that consists of values of 0 and 1, the water was selected and given a value of 0 and the rest of the image a value of 1. When the mask is used in a processing function, such as a supervised classification, ENVI will include areas with values of 1 and ignore the masked 0 values in the calculations.

The training site data for the supervised classification were chosen for three information classes: (1) Active Sand, (2) Dense Vegetation, and (3) Sparse Vegetation on the CCNS landscape. Active sand is defined as sand that is not stabilized by any species of vegetation and vulnerable to aeolian erosion. Dense vegetation is defined as shrubbery, pine forests, or dense patches of grassy species (such as *Ammophila breviligulata*).

Sparse vegetation was defined as areas of the landscape that were sparsely vegetated by grassy species (such as *Ammophila breviligulata*). All of these classes had specific colour values and were readily identifiable in the air photos. Once the training sites were chosen for each information class, the accuracy of the training sites was analyzed.

The first method used to analyze how accurate the training sites were was the n-D visualizer in ENVI 4.2. The n-D visualizer showed the distribution of pixels within and between the training sites. The n-D visualizer is useful for checking the separability of the selected classes. The second method was Computer Training Site Separability report. This computes the spectral separability between selected training site pairs and range from a value of 0 – 2.0. When the value is greater than 1.9, this indicates good separability and the training sites were accepted (ENVI, 2012). Once the separability of the training sites was acceptable using both testing methods, the supervised classification was run for each series of images using the masks. After each supervised classification run, a post classification statistics routine was executed to output the number pixels in each class and the percentage of image surface for each information class.

3.3.5 Velocity Threshold

The threshold velocity for sand transport was calculated using Bagnold's (1941) formula per steps described by Hugenholtz *et al.* (2009). First, the impact threshold shear velocity was calculated using:

$$(1) \quad u_{*t} = A \sqrt{\frac{(\rho_p - \rho_a)gd}{\rho_a}}$$

where, A is an empirical coefficient for the impact threshold (0.08), ρ_p is the density of (assumed quartz) sand particles ($2.65 \times 10^3 \text{ kg m}^{-3}$), ρ_a is air density (1.22 kg m^{-3}), g is gravitational acceleration (9.81 m s^{-2}), and d is the average grain diameter ($5.5 \times 10^{-4} \text{ m}$) determined from samples collected within the Provincelands dune field in CCNS. These values give an impact threshold shear velocity of 0.274 m s^{-1} .

Then the normal velocity $V_t(z)$ was calculated at the station height (z) of 10 meters using the following formula:

$$(2) \quad v_t(z) = \frac{u_{*t}}{\kappa} \ln\left(\frac{z}{z_0}\right) \quad \text{if } z > z_0$$

Where u_{*t} is the impact threshold shear velocity determined from equation (1), κ is von Karman's constant (0.4), Z_0 is aerodynamic roughness length ($8.33 \times 10^{-6} \text{ m}$) for relatively flat sand surfaces derived from grain diameter, $d/30$. These values give a velocity threshold for sand transport of approximately 9.6 m s^{-1} . This value was used to calculate the percentage of winds above the velocity threshold in each year to compare against volumetric changes in corresponding years.

3.4 Results

3.4.1 Volumetric Change

Table 11 shows a summary of the volumetric change that was output from GCD and additional rate calculations that normalizes the changes through time. The volumes and rates of change for erosion and deposition overall seem to be greatest between 1998-2000, then 2000-20007, followed by 2007-2010. This pattern occurs for most individual blowouts in the sub-population. Blowouts 1, 6, 7, 8, 9 and 10 experienced the highest

rates of net erosion in the 1998 to 2000 period. Blowouts 3, 4, and 5 experienced the highest rates of net erosion in 2000-2007, while blowout 2 experienced the highest rate of net erosion in 2007-2010.

Blowout ID	Vol Δ 98 – 00[m ³ (m ³ yr ⁻¹)]			Vol Δ 00-07[m ³ (m ³ yr ⁻¹)]			Vol Δ 07-10 m ³ (m ³ yr ⁻¹)]			TotalΔ98-10[m ³ (m ³ yr ⁻¹)]		
	Eros (rate)	Depo (rate)	Net (rate)	Eros (rate)	Depo (rate)	Net (rate)	Eros (rate)	Depo (rate)	Net (rate)	Eros (rate)	Depo (rate)	Net (rate)
Total (All 10)	-3532 (-1766)	413 (207)	-3119 (-1560)	-11,796 (-1685)	3291 (470)	-8505 (-1214)	-4634 (-1544)	1379 (460)	-3254 (-1085)	-19,962 (-1664)	5083 (423)	-14,876 (-1144)
#1	-1389 (-695)	225 (113)	-1164 (-582)	-3165 (-452)	1072 (153)	-2093 (-299)	-560 (-187)	17 (6)	-543 (-181)	-5114 (-426)	1314 (110)	-3800 (-316)
#2	-259 (-130)	122 (61)	-137 (-68.5)	-1648 (-206)	238 (34)	-1410 (-201)	-1314 (-438)	144 (48)	-1170 (-390)	-3221 (-268)	504 (42)	-2717 (-226)
#3	-866 (-433)	32 (16)	-834 (-417)	-3668 (-524)	1487 (495)	-2181 (-311)	-1401 (-467)	522 (174)	-879 (-293)	-5935 (-494)	2041 (170)	-3894 (-325)
#4	-50 (-25)	12 (6)	-38 (-19)	-485 (-69)	12 (2)	-473 (-68)	-47 (-16)	16 (5)	-31 (-10)	-582 (-49)	40 (3)	-542 (-45)
#5	-94 (-47)	1 (0.5)	-93 (-46.5)	-666 (-95)	10 (1)	-656 (-94)	-205 (68)	7 (2)	-201 (-67)	-965 (-80)	18 (1.5)	-947 (-79)
#6	-169 (-85)	0	-169 (-85)	-505 (-72)	37 (5)	-468 (-67)	-11 (-4)	0	-11 (-4)	-685 (-57)	37 (3)	-648 (-54)
#7	-45 (-23)	3 (1.5)	-61 (-30.5)	-57 (-8)	1 (0.1)	-56 (-8)	-29 (-9)	104 (26)	75 (25)	-131 (-11)	108 (9)	-28 (-2)
#8	-206 (-103)	18 (9)	-188 (-94)	-574 (-82)	225 (32)	-349 (-50)	-187 (-62)	83 (35)	-104 (-35)	-967 (-81)	326 (27)	-641 (-53)
#9	-64 (-32)	1 (0.5)	-44 (-22)	-61 (-9)	1 (0.1)	-60 (-9)	-5 (-2)	16 (5)	11 (3)	-130 (-11)	18 (1.5)	-112 (-9)
#10	-390 (-195)	0	-390 (-195)	-967 (-138)	208 (29)	-759 (-108)	-875 (-292)	470 (157)	-405 (-135)	-2232 (-186)	678 (56.5)	-1554 (-130)

Table 11. A summary of the change in volume (m³) as erosion (Eros, -ve values) or deposition (Depo, +ve values) and rate of volumetric change (m³ yr⁻¹) for the subpopulation of 10 blowouts. The greatest rate of net change in volume for all blowouts combined occurred during the 1998-2000 interval, closely followed by the 2000-2007 interval.

Table 12 is a summary of the V:A (total erosion volume / the total expansion area) of the individual blowouts for each time period. This ratio compares the changes in blowout volume to the expansion of the lateral walls. The values in this table show that there are three ways that blowouts are developing in CCNS. As shown by blowout #10 in 2007-2010 (and others), blowouts can experience change in volume with minimal change to the lateral walls. Blowouts can also expand in area without a great change in volume, as evidenced by the V:A value of blowout # 4 in 1998-2000 (and others). Finally, blowouts in CCNS, such as blowout #10 in 1998-2000, can simultaneously experience areal expansion and deepening.

Blowout ID	1998-2000 V:A (Total Volume m ³ /Total Area m ²)	2000-2007 V:A (Total Volume m ³ /Total Area m ²)	2007-2010 V:A (Total Volume m ³ /Total Area m ²)
#1	12.2 (1389 / 114)	4.0 (3165 / 786)	1.3 (560 / 422)
#2	1.5 (259 / 177)	16.0 (1648 / 103)	5.1 (1314 / 259)
#3	3.8 (866 / 231)	7.3 (3668 / 505)	6.1 (1401 / 230)
#4	0.1 (50 / 442)	2.1 (485 / 232)	0.1 (47 / 401)
#5	0.2 (94 / 429)	0.7 (666 / 968)	2.4 (205 / 86)
#6	14.4 (169 / 12)	2.8 (505 / 181)	0.2 (11 / 47)
#7	0.8 (45 / 59)	0.3 (57 / 205)	2.2 (29 / 13)
#8	2.6 (206 / 78)	14.6 (574 / 39)	1.0 (187 / 180)
#9	1.5 (64 / 43)	1.7 (61 / 37)	0.3 (5 / 16)
#10	1.1 (390 / 357)	2.9 (967 / 376)	43.7 (875 / 20)

Table 12. A summary of the V:A ratio for each year and each blowout in the selected sub-population. The volume change was calculated using GCD and the area of expansion was calculated by a differencing of digitized polygons in ArcGIS. These values show that there are instances where blowouts can deepen with minimal change to the lateral walls (e.g. #10 in 2007-2010), expand in area without deepening (e.g. #4 in 1998-2000), as well as both deepen and expand simultaneously (e.g. #10 in 1998-2000).

Figures 2 through 4 show visual examples and calculated results from GCD. The greatest net rate of erosion for this blowout sub-population occurred between 1998-2000. These changes may be related to the passage of some large tropical storm events, two of which closely followed each other. This was closely followed by 2000-2007, which also experienced tropical storms. Figure 18 displays a pre-existing blowout that continues to develop both in area and volume over time (as captured by the V:A ratio). During the 2000-2007 period, a new blowout was initiated and developed within the area of the examined blowout (Figure 18 - seen in the bottom right corner of the GCD image).

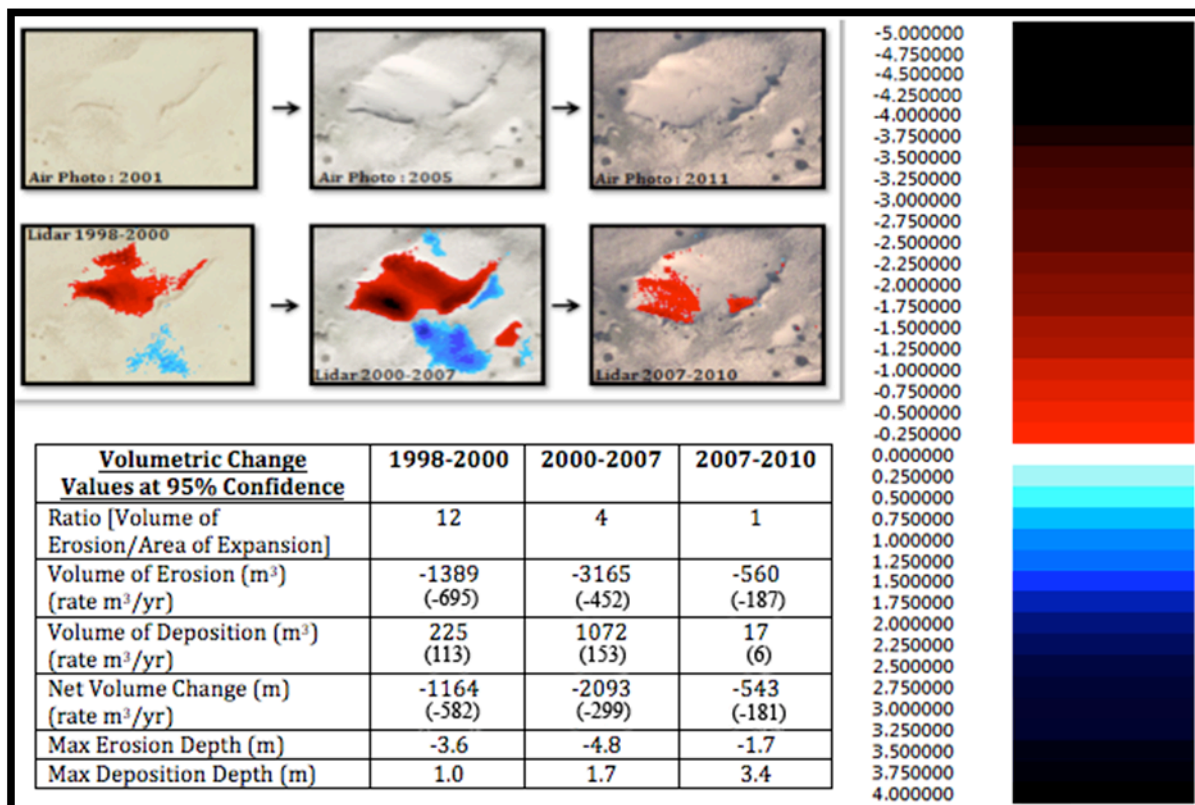


Figure 18. An example of a blowout (not included in sub-population) generation between 2000-2007 (bottom right corner of air photo), and development of a pre-existing blowout (#1). The V:A ratio shows that the greatest erosion occurred between 1998-2000

Figure 19 displays the development of two individual blowouts merging into one larger feature, known as a union event (cf. Abhar *et al.*, 2014, in review). The merging of the two features occurs between 2000 and 2007. This merging or joining of blowouts (a common feature of the Cape blowouts) creates a greater volumetric change in this period, and only slightly lower rate than the change experienced in the 1998-2000 period (85 vs 72 m³ yr⁻¹ rate of erosion; see table embedded in Figure 19). The blowout continues to develop between 2007-2010, however at a slower rate than previous years.

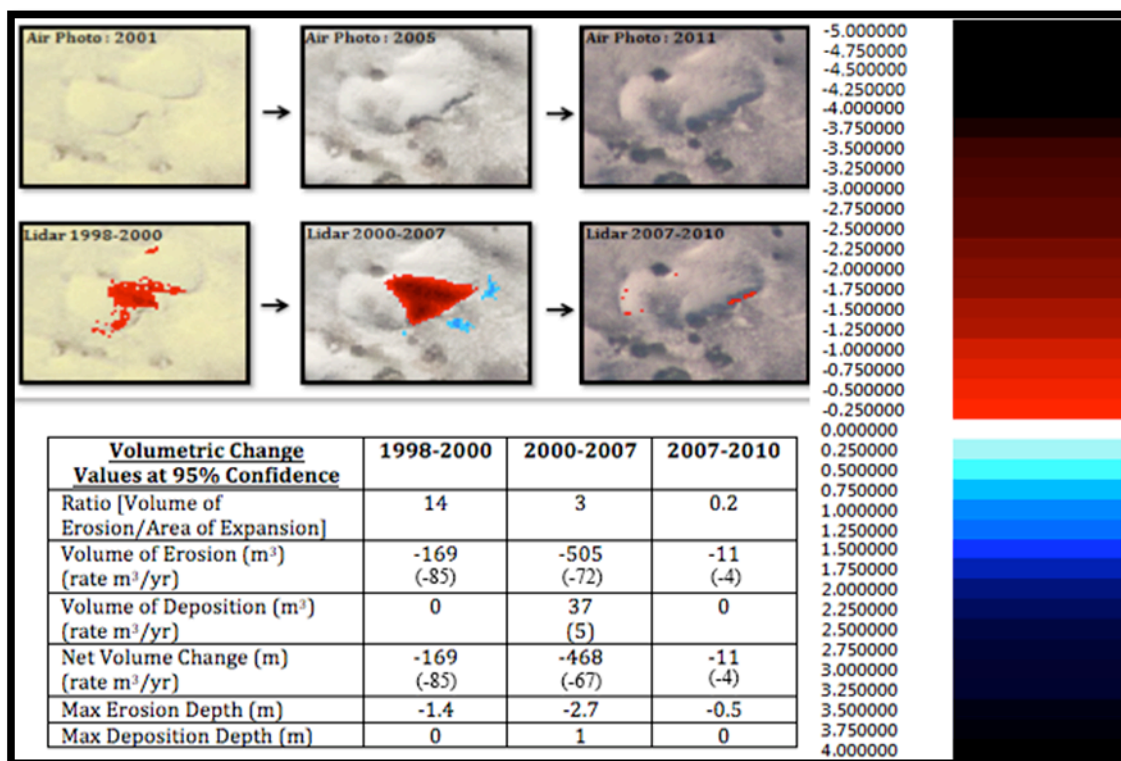


Figure 19. An example of a union event where multiple blowouts (#6) expand into one larger feature (examples seen in STAMP 2D analysis of CCNS blowouts (Abhar *et al.*, 2014). The union event occurs sometime between 2000-2007, which again shows the greatest degree of total change (erosion plus deposition rates) potentially due to Hurricane Noel. (Red = Erosion and Blue = Deposition).

Figure 20 depicts development where the blowout erosional hollow deepens without a significant change in area, followed by an expansion of the blowout's area in subsequent years. Between 1998 and 2000, the blowout experiences the greatest volume of erosion and minimal change in area of expansion, as seen by the relatively high V:A ratio value (see values in Table and Figure 20). It had a similar rate of erosion (103 vs 82 m³ yr⁻¹ rate) in 2000-2007 compared to 1998-2000 (table embedded in Figure 20), but a significantly greater amount and rate of deposition (32 vs 9 m³ yr⁻¹). Between 2007 and 2010, the V:A ratio is a larger value, which indicates that the blowout had a greater volumetric and experienced minimal area change (see values in Figure 20). In the following interval between 2007 and 2010, however, the ratio decreases and it is evident that the blowout experienced change in both area and volume.

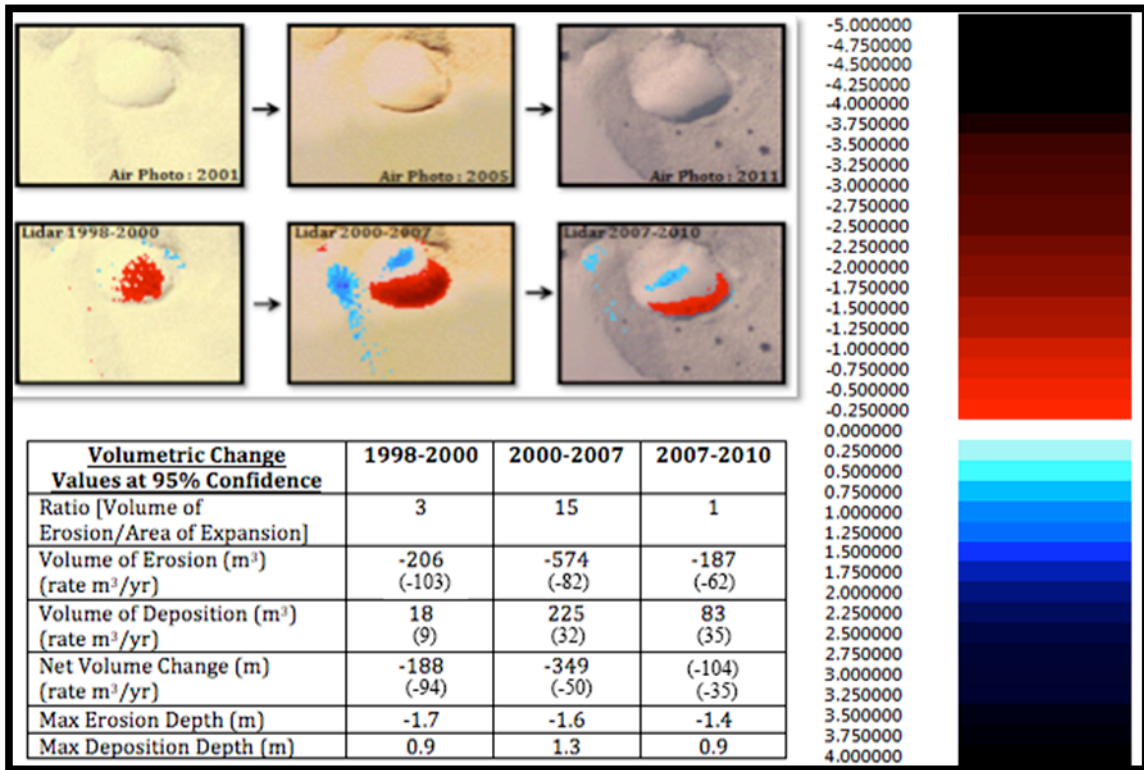


Figure 20. An example of a blowout (#8) increasing in depth, but not in area in 2000-2007. In 2007-2010, however, the feature experiences an increase in area. (Red = Erosion and Blue = Deposition).

3.4.2 Vegetation Change

Figure 21 is a graph showing the percentage of active sands, dense vegetation, and sparse vegetation in the Provincelands as calculated from a supervised classification (as described in section 3.2.3). The general trend shown in the graph is that the active sand cover reduces over time, where the dense and sparse vegetation cover increase over time in the study area.

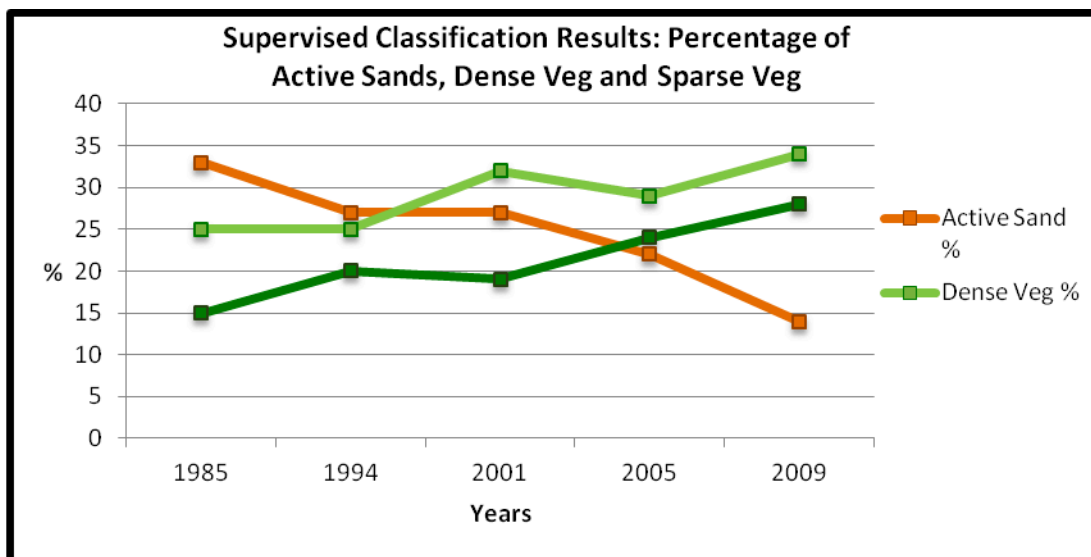


Figure 21. Percentage of surface classified as active sand, sparse vegetation (grassy/ammophila), and dense vegetation (shrubs and trees) as calculated by a supervised classification in ENVI. Over time there is a decrease in active sand surfaces, where the dense and sparse vegetation increase.

3.4.3 Wind Patterns

Figure 22 is a graph showing the percentage of winds recorded from 1998 to 2010 that are above the threshold velocity (9.6 m s^{-1}), which was calculated using Bagnold's equation (1941). The results show that the greatest percentages of winds above 9.6 m s^{-1} are in 2007 and 2010, which coincide with the periods when Hurricanes Noel (3 November 2007) and Earl (4 September 2010) occurred. High wind periods also occurred in 1998 and 1999, which coincide with Hurricanes Bonnie (24 August 1998) and Floyd (17 and 18 September 1999). The high wind periods correspond to years with the highest mean rates of erosion (blowouts # 1, 6, 7, 8, 9, and 10 in 1998-2000, and blowouts # 3, 4, 5 and 6 in 2000-2007) as seen in Table 11, and greatest changes in the ratio of volumetric to area change as seen in blowout number (#8) in Figure 20.

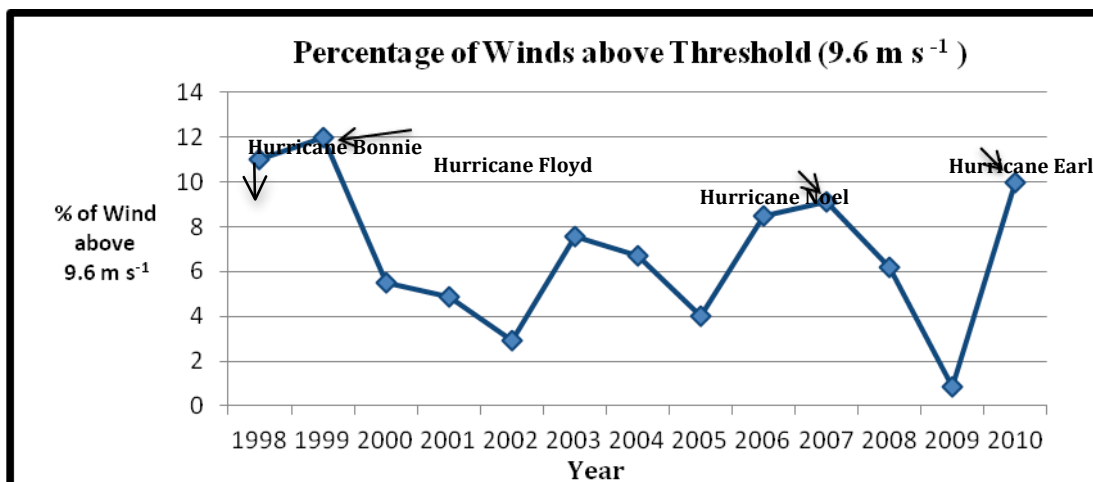


Figure 22. The percentage of wind data above the Bagnold derived threshold of 9.6 m s^{-1} graphed for each year. Hurricane years of 1998 and 1999 had the greatest percentage of competent winds, followed closely by 2007 and 2010. These periods correspond with the greatest rates of erosion of blowouts in the 10 blowouts measured in the Cape Cod region.

3.5 Discussion

3.5.1 Observed morphological and volumetric changes in blowouts of CCNS

Blowout development and evolution is not completely understood and only a few studies that have attempted to present evolutionary models or steps (e.g., Gares and Nordstrom, 1995; Hesp, 2002; Abhar *et al.*, 2014). From the results of the volumetric and area changes computed from the sub-population of ten blowouts in CCNS documented here, there are five patterns of change that were observed: (1) generation (2) areal (or spatial) and volumetric expansion (3) joining of double or multiple blowouts (4) volumetric increase with minimal area change (5) expansion of area. Chapter 2.0 also detected three of these patterns of change (1, 3, and 5) in a spatial-temporal study of a sub-population of 30 blowouts in CCNS. Therefore these results are consistent with those from a larger sub-population.

The generation of blowouts occurs when vegetated sand deposits are exposed to an initiating disturbance followed by high and/or repeated wind erosion that continue the development of the landform (Gares and Nordstrom, 1995; Hesp, 2002). As seen in Figure 18, the geomorphic change detection results also capture the generation of new blowouts. Over time, both erosional and depositional features expanded in area and depth. The variation in the rates of expansion are related to various factors at a landscape scale including increase or decreases in wind speed, precipitation, anthropogenic disturbances, and presence of vegetation (e.g., Hesp, 2002). For instance, the joining of multiple blowouts into one larger feature (e.g., Figure 19) can be a result of intensive scouring of the area between the two closely positioned blowouts. This step in the evolution of blowouts occurs over time to various blowouts in the landscape, as documented also in Chapter 2.0 in a broader spatial-temporal assessment.

The results seen in Figure 20, where between 2000 and 2007 the erosional feature deepens with minimal change to area, would have not been detected without a combination of areal and volumetric analysis. Therefore, blowouts can be static in area while still deepening via wind scouring of sediment in the deflation basin (Figure 20). The same blowout then increased in area between 2007 and 2010, which occurs via expansion of the lateral walls. Therefore, blowouts can potentially have three types of expansion and/or deepening mechanisms (as seen in V:A ratios in Table 12): (1) erosion and expansion of lateral walls (areal change) with minimal change in volume, (2) erosion and deepening of the deflation basin (volumetric) with minimal change in area, (3) or simultaneous erosion of the deflation basin and lateral walls in both area and volume.

The GCD analysis (Table 11) reveals an interesting pattern in the sediment mass balance of the blowouts. Generally, the volume of erosion is greater than the volume of deposition within the domain of analysis for all ten blowouts. As such, there appears to be a negative sediment mass balance for the blowouts. It is likely, however, that appreciable amounts of sediment are being transported well beyond the depositional lobes of the blowouts (i.e., outside of the domain of analysis) and could be feeding the large migrating parabolic dunes in the Provincelands region of CCNS. Forman et al. (2008) examined historic aerial photograph coverage of 11 large parabolic dunes in the same region between 1938 and 2003 and found that, on average, these dunes were migrating downwind at 4 m/yr and increasing in areal extent. Further analysis of landscape-scale volumetric changes could be explored to support the hypothesis that the erosional mass balance of the blowouts is contributing to the volumetric change and resulting migration of the parabolic dunes

3.5.2 Drivers of Blowout Development in CCNS

The morphological evolution of blowouts follows various stages that may not occur in a linear progression (Abhar *et al.*, 2014, in review), but the patterns do depend mainly on certain key factors. These include dominant wind direction, speed, and extreme events, and vegetation cover (presence, absence, density, and species) (e.g. Jungerius and van der Meulen, 1988; Gares, 1992; Gares and Nordstrom, 1995; Hesp and Hyde, 1996; Hesp, 2002; Hugenholtz and Wolfe, 2009; Smyth *et al.*, 2012, 2013).

3.5.2.1 Frequency and magnitude of wind events

Wind direction, speed and extreme wind events are important factors that control blowout size, shape, and direction (Landsberg, 1956; Cooper, 1958; Jungerius *et al.*,

1981; Gares and Nordstrom, 1995; Hesp, 2002; Smyth *et al.*, 2012, 2013; Hesp and Walker, 2013). For instance, Jungerius *et al.* (1991) documented that a shift in dominant wind direction and speed could alter the shape of blowouts toward the directions of the strongest winds. From Figure 22, it is evident that in 1998, 1999, 2007 and 2010 there are peaks in the occurrence of competent winds (i.e., those exceeding the velocity threshold of 9.6 m s^{-1}).

Of the ten selected blowouts, six experienced the greatest erosion rates in the 1998 to 2000 period. On August 24th, 1998, Hurricane Bonnie, then Tropical Storm Bonnie tracked right along the Cape. The wind speed data at the Provincetown wind station showed a high of 15 m s^{-1} (hourly average) and there were 20 hours (3am to 10pm) where the hourly average winds were above the velocity threshold. In the following year, on September 17th and 18th 1999, Hurricane Floyd became a Tropical Storm that traversed right across the Cape with winds approaching hurricane force in Massachusetts (NOAA reports). The wind speed data from the Provincetown wind station showed a high of 15 m s^{-1} (hourly average) and there were 24 hours (2am on the 17th to 12pm on the 18th) where the hourly average winds were above the velocity threshold.

During the 2000-2007 period, four of the blowouts experienced the greatest erosion rates. On 3 November 2007, Hurricane Noel hit the coast of Massachusetts as a Tropical Storm and according to NASA (2007) produced gusts of 35 m s^{-1} at Cape Cod. The wind speed data at the Provincetown wind station showed a high of 19.5 m s^{-1} (hourly average) and there were 13 hours (10am to 12am) where hourly averaged winds were above the velocity threshold. The geomorphic change results (Table 11, Figures 2-5) show greatest net areal and volumetric changes between 2000 and 2007. During this

time, new blowouts were generated (Figure 18), blowouts merged (Figure 19), and the greatest rates and amounts of volumetric change occurred (Figure 18, 19, and 20).

Between 2007 and 2010, there were also high wind events, where one of the ten blowouts had the greatest rate of erosion. On 4th September 2010, (another) Hurricane Earl became a Tropical Storm and brought winds that reached gusts of 30 m s^{-1} (NASA, 2010) near the Cape. The hourly wind speed data from the Provincetown wind station showed a high of 13 m/s^{-1} (hourly average) and there were 10 hours (5am to 3pm) where hourly averaged winds were above the velocity threshold. During this time there continued to be high volumetric changes, however, compared to previous years there was an increase in areal changes as well, as seen from the lower V:A ratio values in Table 12.

From the erosion rates and changes seen in the landscape and the corresponding tropical storm and high wind events in 1998, 1999, 2007 and 2010, there is a high potential for many of these changes to have taken place during these events. It is important to note that these are not the only tropical storms that occurred from 1998 to 2010, as there is an Atlantic Hurricane Season that produces numerous hurricanes that move north of the tropics. However, the aforementioned hurricanes did occur on La Niña years, which again cause hurricanes and tropical storms that are more intense, frequent and probable of landfall in the New England region, and as stated, the Provincetown hourly average wind data shows that these events caused the highest winds in CCNS. Jungerius *et al.* (1991) suggested that the effects of extreme events on blowouts are minor compared to events with lower magnitude and high frequency. However, in CCNS, as seen by the aforementioned examples, the expansion of features appears to occur at a relatively fast pace and within a shorter period of time, potentially within one high wind

event. In addition, although it is difficult to attribute most of the change seen at CCNS in two (1998-2000), seven (2000-2007) and three (2007-2010) years to a single, or series of storm events, the percentages of competent winds are greatest in these years (Figure 22). The average percentage of competent winds from 2000 was 5.5% compared to hurricane years 1998 with and 1999 with; the average of 2000-2006 was 6.1% compared to hurricane year 2007 at 9.1%; and the average of 2007-2009 was 3.6% compared to 2010 at 10%. This shows that the years leading up to the 2007 and 2010 (hurricane years) had less competent winds, as well. Therefore, there is the possibility of multiple high wind events (i.e. hurricanes and storms) occurring at a greater frequency could be driving blowout development. This is especially possible during strong La Niña years (e.g. 1998, 1999, 2007, and 2010), where the frequency and intensity of hurricanes increase (Bove *et al.*, 1998a; Bove *et al.*, 1998b, Pielke and Landsea, 1999; Keim *et al.*, 2004).

It is important, however, to consider that hurricanes often bring precipitation and moisture, which is a stabilizing factor for blowouts (Byrne, 1997; Hesp, 2002). For example, Hurricane Bonnie in 1998 was a slow moving hurricane, which resulted in heavy rainfall during movement through the U.S. (NOAA, 1998). Therefore, the rainfall that stabilizes the sediments in the blowout may offset the sediment transport potential from high winds brought by hurricanes. As described by Zhang *et al.* (2001), there are two major types of storms that affect the East Coast of the U.S.: hurricanes and nor'easters. Although hurricanes are tight and strong low pressure systems that bring high wind speeds, they often influence a small area and (as mentioned) bring heavy rainfall. By contrast, Nor'easters are weaker low pressure systems with peaks in wind that are seldom greater than those of the weakest hurricanes (36 m s⁻¹). However, the wind

speeds are still above the velocity threshold (9.6 m s^{-1}), occur more frequently, are much larger in size, and can occur on days with clear skies (Zhang et al., 2001). Therefore, both hurricanes and nor'easter storms are important components of the competent wind climatology in CCNS that drive blowout morphodynamics. However, further examination of their relative contributions is beyond the scope of this study.

3.5.2.2 Vegetation cover

Vegetation type and density are important factors in all stages of blowout development (Gares and Nordstrom, 1995; Hesp, 2002; Hugenholtz and Wolfe, 2006; Hugenholtz and Wolfe, 2009; Smyth *et al.*, 2012, 2013). For instance, the presence and die-back of vegetation is necessary for the initiation of blowouts as the presence of sparse vegetation sculpts the boundaries of the erosional hollows, and vegetation stabilizes surfaces during the phase of blowouts closure (Gares and Nordstrom, 1995). As seen in Figure 21, the active sand surface in CCNS has decreased over time whilst vegetation cover (both dense and sparse) has increased. Despite these trends, however, blowouts are still generating, increasing in depth, and expanding in area. There are a few potential explanations for these trends. First, a sparsely vegetated surface is conducive to blowout initiation and development (in the case of CCNS with *Ammophila breviligulata*), which allows for the formation of the initial erosional hollow. Therefore, the increase in vegetation, specifically sparse vegetated surfaces, could have created an environment more conducive to blowout initiation. Second, extreme wind events during the intensified La Niña years (as with the hurricanes of 1998, 1999, 2007 and 2010, which were also La Niña years), could cause the burial and removal of vegetation, which leads to a bare surface ideal for blowout initiation (e.g. Figure 23) or areal expansion and volumetric

change of the blowout (e.g. Figure 20). Tsoar (2005) found that high winds are a limiting factor for vegetation on dune sands and that there are thresholds for the destruction of vegetation by storm winds (different for each landscape). Therefore, there is potentially a balance between vegetation and wind interaction on the CCNS landscape that is driving blowout development.



Figure 23. An example of patches of bare sand in CCNS that have formed by vegetation die-back, failure to thrive, or some other currently unknown mechanism. Although there are many factors that could have contributed to the removal of vegetation, or lack of it within a certain patch, high wind events are drivers of vegetation burial and removal. These sparsely vegetated patches, which are widely present on the CCNS landscape, are conducive to blowout initiation. (Image source: Patrick Hesp, October 2012).

3.5.3 Benefits of combining areal and volumetric estimates of geomorphic change

Increasingly, spatial-temporal patterns of change from high resolution digital imagery and/or DEMs are being examined in geomorphology to monitor the evolution of features on varying landscapes, including aeolian blowouts and parabolic dunes (e.g.,

Woolard and Colby, 2002; Mitasova *et al.*, 2005; Dech *et al.*, 2005; Hugenholtz and Wolfe, 2005; Hugenholtz *et al.*, 2009; Hugenholtz and Barchyn, 2010; Mathew *et al.*, 2010; Hugenholtz *et al.*, 2013). As aeolian blowouts can both increase in depth and area over time, it is necessary for any spatial-temporal assessment of their morphology examine resulting volumetric and areal changes. In this study certain patterns of development, such as expansion of the area, and deepening while the area remains stable, were detected by coupling the 2D and 3D analysis. By continuing to approach the study of blowout evolution with both forms of analysis in mind, there will be a more holistic understanding of blowout development on varying landscapes.

3.6 Conclusions

The quantitative analysis of volumetric and areal change of blowouts in CCNS at a landscape scale is examined using airborne LiDAR and air photos. Once DEMs were created for individual blowouts in each sequential year, the DEMs of neighbouring years were differenced for volumetric change analysis using Wheaton *et al.* (2010) GCD software. Areal change was detected by differencing the area of polygons that were manually digitized in ArcGIS. From these analyzes, there were patterns of blowout development that were identified. In order to understand the changes identified in blowouts development in CCNS, further analysis of wind events and patterns, as well as changes in vegetation cover in CCNS were explored.

The results from the GCD and areal change analysis on the selected ten blowouts on CCNS landscape provide the following information on the evolution of these features: (1) blowouts have a point of initiation where an incipient blowout is generated (driven by an initiating factor); (2) multiple blowouts in close proximity can experience areal

expansion, which cause the merging into one often larger feature (also observed in section 2.0); and (3) blowouts can experience deepening of the erosional basin with minimal change to the area of the erosional walls, and vice versa; therefore, blowouts can experience three variations of expansion (listed in section 3.5.1). These areal patterns of change are similar to those identified in section 2.0 when performing spatial-temporal analysis on sequential air photos. However, this study added the

There were two key drivers (wind and vegetation cover) in blowouts development that were analyzed specifically on the CCNS in order to further understand patterns of change detected in the volumetric and areal change analyzes. From these analyzes it was evident that there was significant change that occurred between all the three periods (1998-2000, 2000-2007 and 2007-2010). The percentages of comparable winds (above 9.6 m s^{-1}) were highest in 1998 and 1999, but these were only slightly higher than the 2007 and 2010 years. CCNS experienced several hurricanes during these periods. It is speculated that the significant changes seen in the blowouts of CCNS between 1998-2000, 2000-2007 and 2007-2010 are associated with these extreme wind events. However, it is important to consider that both hurricanes and nor'easters are storm systems that are affecting the CCNS. Furthermore, due to high amounts of rainfall that accompany hurricanes that can stabilize blowout sediment, potentially nor'easters may move more sediment. In addition, supervised classifications were run on sequential air photos of the CCNS landscape. The results indicated an increase in vegetation cover and decrease of active sands over time. There were two potential explanations that were presented as to how the increase in vegetation is related to blowout development: (1) the increase in sparse vegetation created a more conducive environment for the initiation of

blowouts, as this provides stability for the lateral walls, and (2) strong and high wind events (e.g. hurricanes) could have resulted in vegetation burial or die-back allowing for areas of exposed sand for blowout initiation and development.

In considering both the telling results of the volumetric and areal changes, as well as speculations made from wind and vegetation analyzes in relation to blowout development in this study, there is potential for future research and further examination.

(1) Are the patterns of blowout development that have been identified by volumetric and areal analysis occurring on landscapes other than CCNS? (2) In this study there was a lower temporal resolution (since there was limited historical LiDAR for CCNS), which did not allow for year to year examination of the landscape. If the sequential LiDAR and air photos were yearly intervals, changes in the landscape and blowouts could more readily be attributed to hurricanes and landscape changes (e.g. vegetation die-back), or not. (3) By increasing the temporal resolution there may also be achieved a better understanding of the different affects that La Niña and El Niño years have on the CCNS landscape and blowouts.

4.0 Conclusion

4.1 Summary and Conclusion

This thesis presents and implements new methodologies for accurately quantifying geomorphic change in blowouts at a landscape scale. The data used for both independent studies are typical to the coastal geomorphology (LiDAR and orthorectified air photos). While chapter 2.0 focuses on the areal patterns of change, chapter 3.0 aims to understand the evolution of blowouts in CCNS by investigating both volumetric and areal changes.

In Chapter 2.0, the spatial-temporal patterns of blowout populations in CCNS at a landscape scale are identified and quantified using STAMP (Robertson *et al.*, 2007) and additional computations. By running neighbouring year polygon layers of digitized blowouts, STAMP computes population numbers over time, computes shape metrics, classifies and computes the area of geometric and movement events for each year pair, the area of expansion by cardinal direction, and classifies union and division events.

The results from STAMP and the additional computations on the blowouts of CCNS provide the following information on the evolution of these features: (1) both geometric and movement events occur for blowouts in this landscape as they develop; (2) the generation of blowouts in CCNS is greatest in 1985, which by reviewing NPS reports, is potentially related to a coupling of intense vegetation planting campaigns followed by vegetation-dieback (leaving local, sparsely vegetated surfaces); (3) from the three roses (wind, sediment transport, and STAMP) it is evident that these features are expanding and sediment is being transported towards the dominant winds from the North West and the South West; (5) the shape metric shows that the erosional and depositional features

are generally becoming more circular as they develop, which is potentially a result of the multidirectional wind regime; (6) the evolution of these features follow a similar pattern to that described by Gares and Nordstrom's Cyclic Blowouts Evolution Model with two additional stages and one stage modification: union and division events can occur as the features expand and stabilize, as well re-activation events can occur when there is an initiating factor present (e.g. strong winds, storm event, human disturbance, vegetation die-back, etc.).

In Chapter 3.0, the quantitative analysis of volumetric and areal change of blowouts in CCNS at a landscape scale is examined using airborne LiDAR and air photos. The DEMs of neighboring years were differenced for volumetric change analysis using Wheaton *et al.* (2010) GCD software. Areal change was detected by differencing the area of polygons that were manually digitized in ArcGIS. From these analyzes, there were patterns of blowout development that were identified. In order to understand the changes identified in blowouts development in CCNS, further analysis of wind events and patterns, as well as changes in vegetation cover in CCNS were explored.

The results from the GCD and areal change analysis on the selected ten blowouts on CCNS landscape provide the following information on the evolution of these features: (1) blowouts have a point of initiation where an incipient blowout is generated (driven by an initiating force); (2) multiple blowouts in close proximity can experience areal expansion, which causes the merging into one, often larger, feature; (3) blowouts can experience deepening of the erosional basin with minimal change to the area of the erosional walls, and vice versa; (4) and blowouts can experience three variations of expansion: (i) erosion and expansion of lateral walls (area), (ii) erosion and deepening of

the deflation basin (volumetric), (iii) or simultaneous erosion of the deflation basin in both area and volume. These areal patterns of change are similar to those in Chapter 2.0. There were two key drivers (wind and vegetation cover) in blowout development that were analyzed to further understand patterns of change detected in the volumetric and areal change analyzes. The percentages of comparable winds (above 9.6 m s^{-1}) were highest in 1998 and 1999, but these were only slightly higher than the 2007 and 2010 years. CCNS experienced several tropical storms during these periods. It is speculated that the significant changes seen in the blowouts of CCNS between 1998-2000, 2000-2007 and 2007-2010 are associated with these extreme wind events. However, it is important to consider that both hurricanes and nor'easters are storm systems that are affecting the CCNS. Furthermore, due to high amounts of rainfall that accompany hurricanes that can stabilize blowout sediment, potentially nor'easters storms may move more sediment. In addition, supervised classifications were run on sequential air photos of the CCNS landscape. The results indicated an increase in vegetation cover and decrease of active sands over time. There were two potential explanations that were presented as to how the increase in vegetation is related to blowout development: (1) the increase in sparse vegetation created a more conducive environment for the initiation of blowouts, as this provides stability for the lateral walls, and (2) strong and high wind events (e.g. tropical storms) could have resulted in vegetation burial or die-back allowing for areas of exposed sand for blowout initiation and development.

4.2 Research contributions and future work

The major contributions of this research are: (1) the use of new and repeatable methodologies (STAMP and GCD) to study the evolution of blowouts, and (2) the

identification of blowout patterns of change that further contribute to the understanding and literature on their development and evolution (as outlined and discussed in the section above). STAMP and the additional computations provide information on geometric events, movement patterns, area changes, directional change, and union or division of polygon features (in this case, blowouts). By using GCD, results of volumetric change can be incorporated in the study of blowouts. Both STAMP and GCD are automated, systematic and highly useful methods of researching the spatial, volumetric and temporal patterns of change in blowouts or other coastal landforms at a local and a landscape scale.

Recommendations for when using STAMP to study blowouts are: (1) to couple this 2D analysis with volumetric change analysis (i.e. use GCD) on the population of interest in order to have a more holistic understanding of the changes of landforms and the landscape, (2) compare the directional results to Fryberger and Dean (1979) sediment drift roses and wind roses to link process from sediment transport and wind roses to response from the STAMP roses, (3) a supervised classification can assist in understanding the results in comparison to the changes in the vegetation and bare sand surfaces, and (4) land use change and human activity can potentially explain the blowout changes seen in STAMP results, which can be researched by consulting NPS staff or researching NPS historical reports (i.e. vegetation planting campaigns and history of ORV trails). Although recommendations 1 and 3 were carried out in section 3, however, there is a further recommendation for using GCD or STAMP. When using sequential air photo or LiDAR data, use the highest temporal resolution possible in order to examine the landscape and landform changes year to year, which will allow for a better

understanding of what is causing change on the landscape (e.g. hurricanes, ENSO, anthropogenic impacts, vegetation changes).

Furthermore, recommendations for future research beyond this thesis are:

- (1) to research if the patterns of blowout development that have been identified by volumetric and areal analysis occurring on landscapes other than CCNS,
- (2) To explore the implications of precipitation during storms and high wind events on the development of blowouts
- (3) to increase temporal resolution and further explore effects of La Niña and tropical storms on blowout development in CCNS,
- (4) to further investigate the seasonal changes, die-back, failure to thrive and vegetation planting affects on CCNS blowouts,
- (5) to investigate the impacts of anthropogenic activities on the CCNS landscape and blowouts (i.e. ORV trails, vegetation planting campaigns, trampling, fires, etc).
- (6) to study the role of environmental controls in CCNS, such as seasonality and vegetation type.

Bibliography

- Arens, S.M., 1997. Transport rates and volume changes in a coastal foredune on a Dutch Wadden island. *Journal of Coastal Conservation*. 3, 49 – 56.
- Bailey, S.D., Bristow, C.S., 2004. Migrations of parabolic dunes at Aberffraw, Anglesey, north Wales. *Geomorphology*. 59, 165-174.
- Barchyn, T.E., Hugenholtz, C.H., 2013. Reactivation of supply-limited dunefields from blowouts: A conceptual framework for state characterization. *Geomorphology*.
- Bagnold, R.A., 1941. *The Physics of Blown Sand and Desert Dunes*. Methuen, London.
- Boose, E.R., Chamberlin, K.E., Foster, D.R., 2001. Landscape and regional impacts of hurricanes in New England. *Ecological Monographs*. 71, 27-48.
- Bourke, M.C., 2010. Barchan dune asymmetry: Observations from Mars and Earth. *Icarus*. 205, 183-197.
- Bove, M.C., Elsner, J.B., Landsea, C.W. Niu, X., O'Brien, J.J., 1998a. Effect of El Niño on U.S. landfalling hurricanes revisited. *Bulletin of the American Meteorological Society*. 79, 2477-2482.
- Bove, M.C., Sierden D.F., O'Brien, J.J. 1998b. Are Gulf landfalling hurricanes getting stronger? *Bulletin of the American Meteorological Society*. 79, 1327-1328.
- Brock, J.C, Wright, C.W., Sallenger A.H., Krabill W.B., Swift R.N., 2002. Basis and methods of NASA Airborne topographic mapper LiDAR surveys for coastal studies *Journal of Coastal Research*. 18, 1–13.
- Burke, Bill: Cape Cod National Seashore Park Historian. Personal Interview. April 30 2012.
- Byrne, M.L., 1997. Seasonal sand transport through a trough blowout at Pinery Provincial Park, Ontario. *Canadian Journal of Earth Sciences*. 34, 1460 – 1466.
- Carter, R.W.G., 1977. The rate and pattern of sediment interchange between beach and dune. In: Tanner, W.F. (Ed.), *Coastal Sedimentology*. Florida State University, Tallahassee, pp. 3 – 34.

- Carter, R.W.G, Hesp, P.A, Nordstrom, K.F., 1990. Erosional landforms in coastal dunes. In: Nordstrom K.F., Psuty, N.P., Carter, R.W.G. (Eds.), *Coastal Dunes: Form and Process*. Wiley, London, pp.217-249. Cooper, W. S., 1958. *The Coastal Sand Dunes of Oregon and Washington*. Geological Society of America Memoir 72. Boulder, Colorado: Geological Society of America.
- Cooper, W. S., 1958. *The Coastal Sand Dunes of Oregon and Washington*. Geological Society of America Memoir 72. Boulder, Colorado: Geological Society of America.
- Darke, I.B., Walker, I.J., Eamer, J.B.R., 2013. Monitoring considerations for a dynamic dune restoration project: Pacific Rim National Park Reserve, British Columbia, Canada. *Earth Surface Processes and Landforms*. 38, 983-993.
- Dech, J.P., Maun, M.A., and Pazner, M.I., 2005. Blowout dynamics on Lake Huron sand dunes: analysis of digital multispectral data from colour airphotos. *Catena*. 60, 165-180.
- Donaldson, Emily, Gretchen Hilyard, and Margie Coffin Brown 2011 Cultural Landscape Report for Dune Shacks of Peaked Hill Bars Historic District, Cape Cod National Seashore, Provincetown and Truro, Massachusetts. Olmsted Center for Landscape Preservation, Boston, MA.
- Eamer, J.B.R, Walker, I.J., 2010. Quantifying sand storage capacity of large woody debris on beaches using LiDAR. *Geomorphology*. 118, 33-47.
- Eamer, JBR, Walker, IJ (2013). Quantifying spatial and temporal trends in beach-dune volumetric changes using spatial statistics. *Geomorphology* 191: 94-108 (DOI:10.1016/j.geomorph.2013.03.005).
- Eamer, JBR, Darke, IB, Walker, IJ (2013). Geomorphic and sediment volume responses of a coastal dune complex following invasive vegetation removal. *Earth Surface Processes & Landforms*. 38(10): 1148-1159 (DOI: 10.1002/esp.3403).
- Ewing, R.C., Kocurek, G., Lake, L.W., 2006. Pattern analysis of dune-field parameters. *Earth Surface Processes and Landforms*. 31, 1176-1191.
- Ewing, R.C., Kocurek, G., 2010. Aeolian dune-field pattern boundary conditions. *Geomorphology*. 114, 175-187.
- Fletcher, C., Rooney, J., Barbee, M., Lim, S., Richmond, B., 2003. Mapping shoreline change using digital orthophotogrammetry on Maui, Hawaii. *Journal of Coastal Research*. 38, 106-124.

- Forman, S.L., Sagintayev, Z., Sultan, M., Smith, S., Becker, R., Margaret, K., Marin, L., 2008. The twentieth-century migration of parabolic dunes and wetland formation at Cape Cod National Sea Shore, Massachusetts, USA: landscape response to a legacy of environmental disturbance. *The Holocene*. 18, 01-10.
- Fryberger, S.G. and Dean, G., 1979. Dune forms and wind regime. In: *A Study of Global Sand Seas* (Ed. E.D. McKee). Geological Survey Professional Paper. 1052, 137–169. Geological Survey, Washington, DC.
- Gares, P.A., 1992. Topographic changes associated with coastal dune blowouts at island beach State Park, NJ. *Earth Surface Processes and Landforms*. 17, 589 - 604.
- Gares, P.A., Nordstrom, K.F., 1995. A cyclic model of foredune blowout evolution for a leeward coast: Island Beach, NJ. *Annals of the Association of American Geographers*. 85, 1 – 20.
- González-Villanueva, R., Coastas, S., Duarte, H., Pérez-Arlucea, M., Alejo, I., 2011. Blowout evolution in a coastal dune: using GPR, aerial imagery and core Records. *Journal of Coastal Research*. 64, 278-282.
- Hesp, P.A., 2002. Foredunes and blowouts: initiation, geomorphology and dynamics. *Geomorphology*. 48, 245-268.
- Hesp, P.A., 2011. Dune Coasts. *Treatise on Estuarine and Coastal Science*, In: Wolanski E. and McLusky D.S. (Eds.), Waltham: Academic Press, pp. 193–221.
- Hesp, P.A., Hyde, R., 1996. Flow dynamics and geomorphology of a trough blowout. *Sedimentology*. 43, 505-525.
- Hesp, P.A., Pringle, A., 2001. Wind flow and topographic steering within a trough blowout. *Journal of Coastal Research*. 34, 597-601.
- Hesp P.A., Walker I.J., 2012. Three-dimensional aeolian dynamics within a bowl blowout during offshore winds: Greenwich Dunes, Prince Edward Island, Canada. *Aeolian Research*, 3, 389-399.
- Hesp, P.A., Walker, I.J., 2013. Coastal Dunes. *Treatise on Geomorphology*. In: John F. Shroder (Eds.). Academic Press, San Diego, pp. 328-355.
- Hugenholtz, C.H., Wolfe, S.A., 2005. Biogeomorphic model of dunefield activation and stabilization on the northern Great Plains. *Geomorphology*. 70, 53-70.
- Hugenholtz, C.H., Wolfe, S.A., 2006. Morphodynamics and climate controls of two aeolian blowouts on the northern Great Plains, Canada. *Earth Surface Processes & Landforms*. 31, 1540-1557.

- Hugenholtz, C.H., Wolfe, S.A., Walker I.J., Moorman, B.J., 2009. Spatial and temporal patterns of aeolian sediment transport on an inland parabolic dune, Bigstick Sand Hills, Saskatchewan, Canada. *Geomorphology*. 105, 158-170.
- Hugenholtz, C.H., Wolfe, S.A., 2009. Form-flow interactions in an aeolian saucer blowout. *Earth Surf. Proc. & Land*. 34, 919-928.
- Hugenholtz, C.H., Barchyn, T.E., 2010. Spatial analysis of sand dunes with a new global topographic dataset: new approaches and opportunities. *Earth Surface Processes & Landforms*. 35, 986-992.
- Hugenholtz C.H., 2010. Topographic changes of a supply-limited inland parabolic sand dune during the incipient phase of stabilization. *Earth Surface Processes & Landforms*. 35, 674-1681.
- Hugenholtz, C.H., Levin, N., Barchyn, T., Baddock, M. 2012. Remote sensing and spatial analysis of aeolian sand dunes: a review and outlook. *Earth-Science Reviews*. 111, 319-334.
- Hugenholtz, C.H., Levin, N., Barchyn, T., Baddock, M., 2012. Remote sensing and spatial analysis of aeolian sand dunes: a review and outlook. *Earth-Science Reviews*. 111, 319-334.
- Houser, C., Hamilton S., 2009. Sensitivity of post-hurricane beach and dune recovery to event frequency. *Earth Surface Processes and Landforms*. 34, 613-628.
- Jungerius, P. D., Verheggen, J. T., Wiggers, A. J., 1981. The Development of Blowouts in 'de Blink' a Coastal Dune Area near Noordwijkerhout, The Netherlands. *Earth Surface Processes and Landforms*. 6, 375-396.
- Jungerius, P.D., van der Meulen, F., 1988. Erosion processes in a dune landscape along the Dutch coast. *Catena*. 15, 217 – 228.
- Jungerius, P.D., van der Meulen, F., 1989. The development of dune blowouts, and measured with erosion pins and sequential air photos. *Catena* 16, 369 – 376.
- Jungerius, P.D., van der Meulen, F., Loedeman, J.H., Stuiver, J., 1992. A geometrical approach to monitoring blowout development from aerial photographs using a Geographical Information System (GIS), in: Carter, R.W.G. *et al.* (Ed.) (1992). *Coastal dunes: geomorphology, ecology and management for conservation: Proceedings of the 3rd European Dune Congress*.
- Kocurek, G., Ewing, R.C., 2005. Aeolian dunefield self-organization – implications for

the formation of simple versus complex dune-field patterns. *Geomorphology*. 72, 94-105.

Landsberg, S.Y., 1956. The Orientation of Dunes in Britain and Denmark in Relation to the Wind. *Geographical Journal*. 122, 176-189.

Massachusetts Office of Geographic Information, 2014. MassGIS Data Layers. Retrieved October 2012 from: <http://www.mass.gov/anf/research-and-tech/it-serv-and-support/application-serv/office-of-geographic-information-massgis/datalayers/layerlist.html>.

Mathew, S., Davidson-Arnott, R.G.D, Ollerhead, J., 2010. Evolution of beach-dune system following a catastrophic storm overwash event: Greenwich Dunes, Prince Edward Island, 1936-2005. *Canadian Journal of Earth Science*. 47(3): 273-290.

Maun, M.A., 1998. Adaptations of plants to burial in coastal sand dunes. *Canadian Journal of Botany*. 76, 713–38.

Melton, F.A., 1940. A tentative classification of sand dunes: its application to dune history in the southern High Plains. *Journal of Geology*. 48, 113 – 174.

Mitasova H, Overton M, Harmon RS., 2005. Geospatial analysis of a coastal sand dunefield evolution: Jockey's Ridge, North Carolina. *Geomorphology*. 72, 204 – 221.

Miller .H.J., Wentz E.A., 2003. Representation and spatial analysis in geographic information systems. *Annals of the Association of American Geographers*. 93, 574–594.

Maun, M.A., Perumal, J., 1999. Zonation of vegetation on lacustrine coastal dunes: effects of burial by sand. *Canadian Journal of Botany*. 2, 14–18.

Moore, L.J., 2000. Shoreline mapping techniques. *Journal of Coastal Research*. 16, 111–124.

NASA., 2014. NASA Hurricanes/ Tropical Cyclones.
http://www.nasa.gov/mission_pages/hurricanes/main/#.Ux1k_GRdX2A

National Climatic Data Center, 2013. NCDC Map viewer. Retrieved October 2013 from: <http://gis.ncdc.noaa.gov/map/viewer/#app=cdo>.

NOAA, 2002. Climatography of the United States No. 81. National Climatic Data Center, pp 16.

NOAA Coastal Services Center, 2014. Digital Coast Data Viewer. Retrieved October 2012 from: <http://www.csc.noaa.gov/digitalcoast/>.

- NOAA, 1998. National Weather Service – Hurricane Bonnie. Retrieved April 19th, 2014 from: <http://www.weather.gov/mhx/Aug271998EventReview>.
- Nordstrom, K.F., Psuty, N.P., Carter, R.W.G., 1990. Coastal Dunes Form and Process. Chichester, New York, John Wiley & Sons.
- Pearce, K.I., Walker, I.J., 2005. Frequency and magnitude biases in the ‘Fryberger’ model, with implications for characterizing geomorphically effective winds. *Geomorphology*. 68, 39-55.
- Pluis, J.L.A., 1992. Relationships between deflation and near surface wind velocity in a coastal dune blowout. *Earth Surface Processes and Landforms*. 17, pp. 663–673.
- Robertson, C., Nelson, T., Boots, B., Wulder, M.A., 2007. STAMP: spatial–temporal analysis of moving polygons. *Journal of Geographical Systems*. 9, 207–227.
- Robertson, C., Nelson, T., Jelinski, D.E., Wulder, M.A., Boots, B., 2009. Spatial–temporal analysis of species range expansion: the case of the mountain pine beetle, *Dendroctonus ponderosae*. *Journal of Biogeography*. 36, 1446-1458.
- Sadahiro Y., Umemura, M., 2001. A computational approach for the analysis of changes in polygon distributions. *Journal of Geographical Systems*. 3, 137–154.
- Sallenger A.H., Krabill W.B., Swift R.N., Brock J., List J., Hansen M., Holman R.A., Manizade S., Sontag J., Meredith A., Morgan K., Yunkel J.K., Frederick E.B., Stockdon H. 2003. Evaluation of airborne topographic LiDAR for quantifying beach changes. *Journal of Coastal Research*. 19, 125–133.
- Saunders, K.E., Davidson-Arnott, R.G.D., 1990. Coastal dune response to natural disturbances. *Proc. Symposium on Coastal Sand Dunes*. NRC, Ottawa, pp. 321 – 345.
- Seppälä M., 1984. Deflation measurement in Hietatievat, Finnish Lapland 1974–77. In *Northern Ecology and Resource Management*, Olson R, Geddes F, Hastings R (Ed.). The University of Alberta Press: Edmonton, Alberta. 39-48.
- Simpson, R.H., Riehl, H., 1981. *The Hurricanes and it’s impact*. Louisiana State University Press, Baton Rouge, Louisiana, USA.
- Stojic, M., Chandler, J.H., Ashmore, P., Luce, J., 1998. The assessment of sediment transport rates by automated digital photogrammetry. *Photogrammetric Engineering and Remote Sensing*. 64, 387–395.

- Smyth, T.A.G., Jackson D.W.T., Cooper, J.A.G., 2012. High resolution measured and modelled three-dimensional airflow over a coastal bowl blowout. *Geomorphology*. 177-178, 62-73.
- Smyth, T.A.G., Jackson D.W.T., Cooper, J.A.G., 2013. Three dimensional airflow patterns within a coastal trough-bowl blowout during fresh breeze to hurricane force winds. *Aeolian Research*. 9, 111-123.
- Timm, B.C., Smith, S.M., Greenspan, S.E. In press. Remotely-sensed mapping of *Ammophila* spp. distribution and density at Cape Cod National Seashore. *Journal of Coastal Research*.
- Tsoar, H., Blumberg, D.G., 2002. Formation of parabolic dunes from barchan and transverse dunes along Israel's Mediterranean coast. *Earth Surface Processes and Landforms*. 27, 1147-1161.
- Walker, IJ, Eamer, JBR, Darke, IB (2013). Assessing significant geomorphic changes and effectiveness of dynamic restoration in a coastal dune ecosystem. *Geomorphology* (DOI: 10.1016/j.geomorph.2013.04.023).
- Wheaton, J., Brasington, J., Darby, S. E., & Sear, D. (2010). Accounting for uncertainty in DEMs from repeat topographic surveys: improved sediment budgets. *Earth Surface Processes and Landforms*, 156: 136–156.
- Woolard, J.W., Colby, J.D., 2002. Spatial characterization, resolution, and volumetric change of coastal dunes using airborne LIDAR: Cape Hatteras, North Carolina: *Geomorphology*. 48, 269-287.
- Zeigler, J.M., Tuttle, S.D., Tasha, H.J., Geise, G.S., 1965. The Age and Development of the Provincelands Hook, Outer Cape Cod, Massachusetts. *Limnology and Oceanography*. 10, 298-311.
- Zhang, K., Douglas, B.C., Letherman, P., 2001. Beach Erosion Potential for Severe Nor'easters. *Journal of Coastal Research*. 17, 309 – 321.